

What Is Mature and What Is Still Emerging in the Cryptocurrency Market?

Stanisław Drożdż ^{1,2,†} , Jarosław Kwapien ^{2,†}  and Marcin Wątopek ^{1,*,†} 

¹ Faculty of Computer Science and Telecommunications, Cracow University of Technology, ul. Warszawska 24, 31-155 Kraków, Poland; stanislaw.drozd@ifj.edu.pl

² Complex Systems Theory Department, Institute of Nuclear Physics, Polish Academy of Sciences, ul. Radzikowskiego 152, 31-342 Kraków, Poland; jaroslaw.kwapien@ifj.edu.pl

* Correspondence: marcin.watorek@pk.edu.pl

† These authors contributed equally to this work.

Abstract: In relation to the traditional financial markets, the cryptocurrency market is a recent invention and the trading dynamics of all its components are readily recorded and stored. This fact opens up a unique opportunity to follow the multidimensional trajectory of its development since inception up to the present time. Several main characteristics commonly recognized as financial stylized facts of mature markets were quantitatively studied here. In particular, it is shown that the return distributions, volatility clustering effects, and even temporal multifractal correlations for a few highest-capitalization cryptocurrencies largely follow those of the well-established financial markets. The smaller cryptocurrencies are somewhat deficient in this regard, however. They are also not as highly cross-correlated among themselves and with other financial markets as the large cryptocurrencies. Quite generally, the volume V impact on price changes R appears to be much stronger on the cryptocurrency market than in the mature stock markets, and scales as $R(V) \sim V^\alpha$ with $\alpha \gtrsim 1$.

Keywords: blockchain; cryptocurrencies; time series; fluctuations; correlations; multifractality; market maturity; market impact



Citation: Drożdż, S.; Kwapien, J.; Wątopek, M. What Is Mature and What Is Still Emerging in the Cryptocurrency Market? *Entropy* **2023**, *25*, 772. <https://doi.org/10.3390/e25050772>

Academic Editor: Marcel Ausloos

Received: 21 April 2023

Revised: 4 May 2023

Accepted: 6 May 2023

Published: 9 May 2023



Copyright: © 2023 by the authors. Licensee MDPI, Basel, Switzerland. This article is an open access article distributed under the terms and conditions of the Creative Commons Attribution (CC BY) license (<https://creativecommons.org/licenses/by/4.0/>).

1. Introduction

Studying the world cryptocurrency market is welcome for many reasons. Up to now, it constitutes the most spectacular and influential application of the distributed ledger technology called the blockchain, which, in the underlying peer-to-peer network, allows for the same access to information for all participants [1,2]. Research on blockchain technology is also unique because all related data are publicly available in the form of the history of every operation performed on the network. Furthermore, the tick-by-tick data for each transaction made on the cryptocurrency exchange are freely available using the application programming interfaces (APIs) of a given exchange.

As far as the financial, economic, and, in general terms, social aspects of cryptocurrencies are concerned, a basic related question that arises is whether such digital products can be considered as a commonly accepted means of exchange [3–5]. This is a complex issue involving many social, economical, and technological factors, such as trust, perceived risk, peer opinions, transaction security, network size effect, supply elasticity, and so on. However, also from a dynamical perspective, for this to apply, a certain level of maturity expressed in terms of market efficiency, liquidity, stability, size, and other characteristics is required [6,7]. Moreover, the developed markets show several statistical properties that newly established emerging markets often lack. Among such properties, one can list the so-called financial stylized facts: heavy tails of the probability distribution functions of fixed-time returns, long-term memory of volatility, a hierarchical structure of the asset cross-correlations, multifractality, and a stable (or meta-stable) price impact function [8–11].

There is growing quantitative evidence that the cryptocurrency market continuously advances on a route to maturity understood as sharing its statistical properties with the traditional financial markets. For instance, the most popular and oldest cryptocurrency, bitcoin (BTC), has passed through two stages of the shaping of its probability distribution function (pdf). It started as an extremely volatile asset with pdf tails that used to decline according to a power law, with the exponent reaching almost the Lévy-stable regime (the Lévy parameter $\alpha \approx 2$) on short time scales over the years 2012–2013, but then, already in the years 2014–2015, the tails of its pdf became thinner and reached the inverse cubic behavior that is observed universally in the traditional financial markets [12]. From that moment on, BTC has maintained this property over the subsequent years [6,13,14]. The difference between BTC and traditional assets is that the inverse cubic behavior of the BTC pdf tails was reported to be preserved up to much longer sampling intervals due to their less frequent trading [12]. Similar effects were seen for other major crypto currencies, such as ETH [12,15]. Since BTC and the other cryptocurrencies are traded on many independent platforms that differ in trading frequency, the pdf properties of the same cryptocurrency can be different on different platforms [6]. This is quite a unique trait of the cryptocurrencies not observed, for example, in the stock markets and Forex. Heavy pdf tails were also found in time series of volume traded in time units [16,17], even in the case of cryptocurrencies [18,19]. These two quantities—the log-returns and volume—are related to each other, because the size of a trade can have a profound impact on price variation: large trades lead to large price jumps on average (although this relation might be more subtle [20–22]). Some authors argue that price impact assumes a functional form with a square-root dependence of the log-returns on volume [23–25] but others are cautious [21,22,26].

The long-term memory of volatility fluctuations is responsible for the effect of volatility clustering, i.e., periods of a volatile market with large-amplitude fluctuations are interwoven with periods of relatively tranquil dynamics. In addition, the volatility autocorrelation is of a power-law form [27]. This property has been seen in all financial markets and has also been found in cryptocurrency dynamics [14]. The range of memory is comparable in this case with the range for the stock and Forex markets [28,29]. The scale-free form of the autocorrelation function is connected to fractality, which also requires long-term or long-range correlations to be self-similar. The log-return fluctuations for all the traditional financial markets studied so far show multiscaling together with some other quantities, such as inter-transaction times [30–32]. Consistently, multifractal properties have been observed in the cryptocurrency market returns and inter-transaction times for different assets [6,18,33–39]. Apart from univariate multiscaling, its bivariate version has also been reported between log-returns for different cryptocurrencies: BTC and ETH [40].

Apart from correlations in time, asset–asset cross-correlations play an important role in the shaping of the financial market structure as they lead to the emergence of the hierarchical organization of the markets as well as coupling between different markets [41–44]. While the hierarchical cross-correlations among the assets traded on the same market are a clear indicator of market maturity, the role of potential couplings between different markets must be interpreted with care. This is because either the independent dynamics of a market or the profound coupling of a market with the world’s leading markets, being the two opposite cases, can potentially be interpreted in favor of market maturity. The former because independence can be viewed as strength and as a possibility for using the assets traded on such a market as a safe haven in hedging strategies [45,46], and the latter because it suggests that such a market is a well-rooted part of global financial markets. However, intuitively, neither of these extremes seems to represent the notion of maturity well enough. It is more justified to view market maturity as the ability to switch its dynamics between independence and compliance because such a behavior can better reflect the complexity that one may expect to be the property characterizing a developed market. This is why neither the effect of the cryptocurrency market decoupling from Forex reported in [29] nor the effects of the cryptocurrency market independence [47–51] and strong coupling between the cryptocurrencies and traditional financial markets reported in [52–55], respectively, can alone be a signature of maturity. It is

rather the opposite: only such flexible dynamics swinging between idiosyncrasy and a strong subjugation of the market to an actual global trend can be a manifestation of market maturity.

In this work, stress was put on the investigation of current statistical properties of cryptocurrency log-returns and volume from the perspective of how these properties differ from their counterparts in the traditional financial markets: the stock markets, Forex, and commodity markets. One has to be aware, however, that the statistical approach constitutes only a segment of the issues related to market maturity.

2. Methods and Results

2.1. Empirical Dataset

The data set studied contains 1 min quotations of 70 cryptocurrencies that were among the most actively traded on the Binance exchange [56], which had the largest market share in 2022 [57], over the period from 1 January 2020 to 31 December 2022 (3 years). The quotes are expressed in USD Tether (USDT), a stablecoin linked to the US dollar, and its value is close to USD 1 by design [58]. Basic time series statistics corresponding to these 70 cryptocurrencies are collected in Table 1. For a time series of price quotations $Q(t_i)$, $i = 1, \dots, T$, the equally spaced logarithmic returns $R_{\Delta t}(t_i) = \log Q(t_i) - \log Q(t_{i-1})$, where $t_i - t_{i-1} = \Delta t$, are derived. Figure 1 shows the evolution of the cumulative log-returns $\hat{R}_{\Delta t}(t_i) = \sum_{i=1}^i R_{\Delta t}(t_i)$ during the whole period covered by the data. In accordance with the actual cryptocurrency price quotes, in 2021, the whole market experienced a transition from the bull phase to the bear phase.

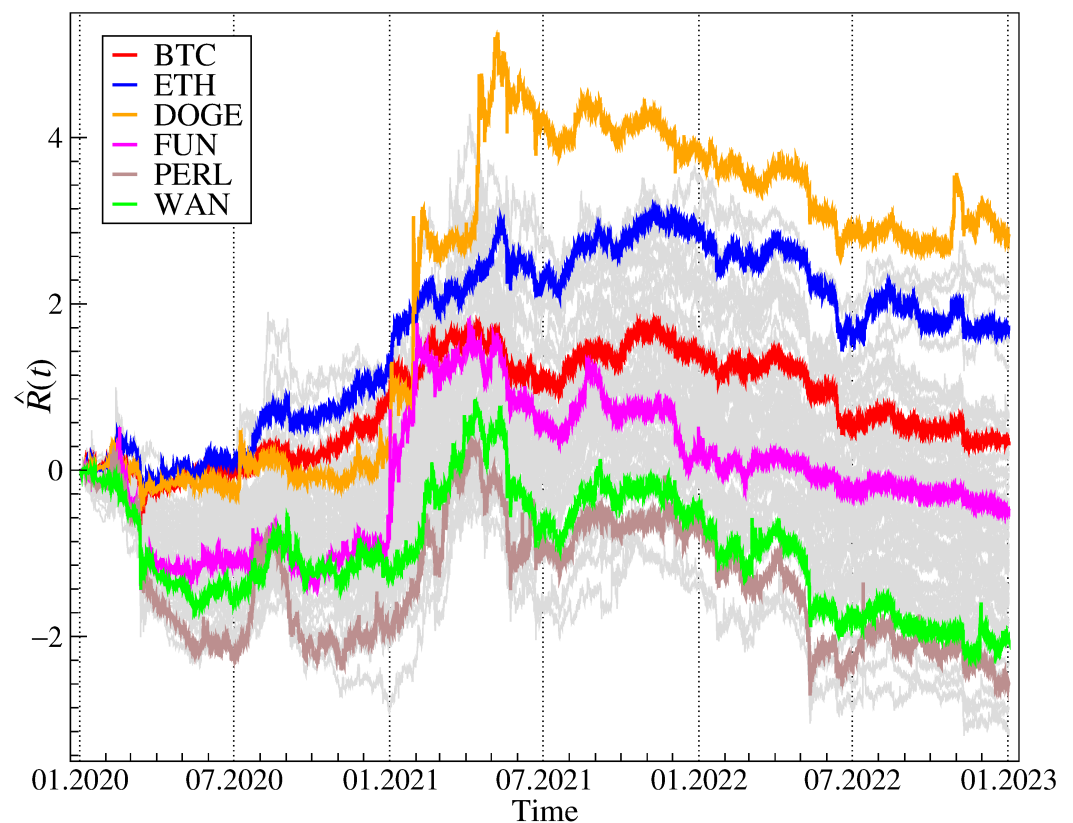


Figure 1. Evolution of the cumulative log-returns $\hat{R}(t)$ of the 70 cryptocurrencies over the time period from 1 January 2020 to 31 December 2022. The colors of two of the most liquid cryptocurrencies and a few other distinguished ones are indicated explicitly. The bulk of the cryptocurrencies is shown in the background (grey lines).

Table 1. Basic statistics of the cryptocurrencies considered in this study: the average inter-transaction time δt , the fraction of zero returns in time series %0, the average volume value traded per minute W , and market capitalization C on 1 January 2023. For the cryptocurrency name list, see Table A1 in Appendix A.

Ticker	δt [s]	%0	W [USDT]	C [$\times 10^6$ USD]	Ticker	δt [s]	%0	W [USDT]	C [$\times 10^6$ USD]
BTC	0.04	0.003	1,683,710	320,025	LINK	0.41	0.095	84,423	2856
ADA	0.24	0.121	172,891	8621	LTC	0.41	0.142	80,441	5096
ALGO	0.78	0.117	24,320	1267	MATIC	0.32	0.166	100,100	6638
ANKR	1.84	0.195	10,762	151	MFT	5.01	0.425	2436	54
ARPA	2.75	0.165	6082	33	MTL	3.16	0.400	5122	46
ATOM	0.58	0.109	42,048	2710	NEO	1.45	0.194	18,893	451
BAND	2.13	0.175	8285	49	NKN	2.99	0.425	5807	56
BAT	1.53	0.162	10,543	251	NULS	4.44	0.442	2845	12
BCH	0.70	0.140	48,288	1869	OMG	0.83	0.178	24,235	146
BEAM	5.30	0.433	2089	14	ONE	0.97	0.227	21,983	133
BNB	0.17	0.095	276,261	39,052	ONG	5.53	0.482	2297	71
CELR	1.77	0.292	10,843	68	ONT	1.28	0.149	16,136	134
CHZ	0.59	0.232	51,827	672	PERL	5.00	0.431	2406	7
COS	2.63	0.455	3575	18	QTUM	1.58	0.179	14,178	196
CTXC	3.42	0.464	3942	33	REN	2.72	0.207	6232	62
DASH	1.44	0.206	14,543	468	RLC	2.80	0.293	6090	95
DENT	1.24	0.353	16,417	68	RVN	1.82	0.202	9699	232
DOCK	5.39	0.455	2135	12	STX	4.42	0.416	3847	288
DOGE	0.20	0.173	247,343	9317	TFUEL	2.09	0.353	10,411	189
DUSK	2.97	0.441	3994	34	THETA	0.64	0.173	35,023	733
ENJ	1.17	0.225	21,114	243	TOMO	3.84	0.316	3581	24
EOS	0.53	0.147	59,616	948	TROY	3.20	0.381	3347	23
ETC	0.58	0.099	63,736	2188	TRX	0.46	0.142	71,306	5041
ETH	0.10	0.010	853,284	146,967	VET	0.52	0.093	55,362	1163
FET	2.65	0.255	7,909	75	VITE	4.22	0.469	3078	18
FTM	0.50	0.174	63,723	556	WAN	7.24	0.303	1609	34
FUN	3.91	0.538	2911	66	WAVES	1.19	0.177	19,265	144
HBAR	1.57	0.268	11,765	957	WIN	1.01	0.283	26,244	72
HOT	0.96	0.237	22,543	250	XLM	0.78	0.165	33,309	1894
ICX	2.64	0.306	6951	135	XMR	1.62	0.184	14,164	2707
IOST	1.40	0.199	14,551	129	XRP	0.21	0.071	229,976	17,055
IOTA	1.53	0.168	12,077	478	XTZ	1.08	0.137	19,407	663
IOTX	1.52	0.266	11,894	203	ZEC	1.15	0.240	20,010	597
KAVA	1.57	0.155	12,888	198	ZIL	1.03	0.145	20,195	258
KEY	2.83	0.358	4310	15	ZRX	3.04	0.214	5674	128

2.2. Cumulative Distribution Functions of Returns and Volume

The cumulative distribution function (cdf) $P(X > r_{\Delta t})$ can be calculated from the normalized returns $r_{\Delta t}(t_i) = (R_{\Delta t}(i) - \mu)/\sigma$, with μ and σ denoting sample mean and standard deviation, respectively. A form of this distribution varies among the markets and assets, but some interesting properties can be observed. There are generally three factors that shape it: the first one is liquidity, the second one is trading speed, and the third one is the overall market volatility [59]. If one focuses on a specific market, the most liquid assets show a faster decline in $P(X > r_{\Delta t})$ with $r_{\Delta t}$ than the less liquid ones for a given Δt [60]. However, most of the assets traded on mature markets reveal a power-law dependence of $P(X > r_{\Delta t})$ for some range of Δt [23,27,60–62]:

$$P(X > r_{\Delta t}) \sim |r_{\Delta t}|^{-\gamma}, \quad (1)$$

with $\gamma \approx 3$. It is observed for short sampling intervals and it is persistent for a range of Δt due to the existence of strong inter-asset correlations. This inverse cubic power-law dependence breaks for sufficiently long Δt and the cdf tails converge to the expected normal distribution. The speed of information processing on a given market also has influence on the crossover Δt . Since this speed increases with time as new technologies enter the service, we observe a gradual decrease in the crossover Δt across decades. The speed of market trading allows for a larger transaction number in time units, so this factor accelerates the market time even more [60]. The emerging markets, where investment strategies require the accommodation of significant risk, are thus highly volatile. The cdfs of the asset returns in this case often show heavy tails with the scaling exponent $\gamma \ll 3$, sometimes even in the Lévy-stable regime. In such markets, the inverse cubic behavior of $P(X > r_{\Delta t})$ may occur for some assets only, whereas, for the other assets, it cannot be found at all. This is why such extreme tails are often considered to be an indicator of market immaturity [14].

Based on the average inter-transaction time δt , we categorized the considered cryptocurrencies into three groups: I, the most frequently traded cryptocurrencies ($\delta t < 1s$); II, the cryptocurrencies with the average trading frequency ($1s \leq \delta t < 2s$); and III, the least frequently traded cryptocurrencies ($\delta t \geq 2s$). Then, we calculated the average cdfs for the cryptocurrencies belonging to each group. We show these cdfs in Figure 2 (left panel, dotted lines) together with the cdfs for a few selected individual cryptocurrencies (solid lines). Their form can be compared with the inverse cubic power-law model denoted by a dashed line. It can be seen that the average distributions have their tail close to a power law, with the exponent γ being close to 3. The most liquid cryptocurrencies—BTC and ETH—develop tails that show a cross-over from the power-law regime to a CLT-like regime for relatively small values of $|r_{\Delta t}|$ compared to both the average cdfs and to less frequently traded individual cryptocurrencies such as FUN, PERL, and WAN. The case of Dogecoin, which has the smallest slope in the middle of the distribution and, at the same time, does not have the thickest tail, is special. On the one hand, it can be included among the main cryptocurrencies due to the high frequency of transactions and capitalization, and, on the other, it was the subject of possible price manipulation through Elon Musk's tweets [63,64].

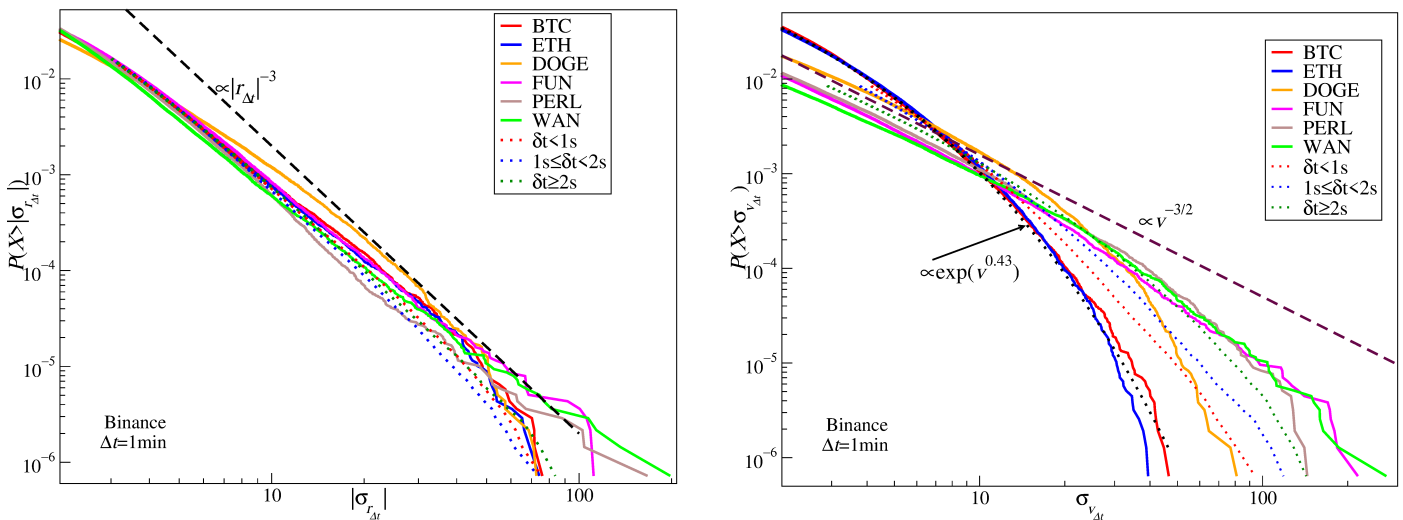


Figure 2. Cumulative distribution functions of the absolute normalized log-returns $r_{\Delta t}$ (left) and the normalized volume traded $v_{\Delta t}$ (right) for $\Delta t = 1 \text{ min}$ in units of the respective standard deviations σ for the selected cryptocurrencies with the highest liquidity (BTC and ETH) or the heaviest tails (DOGE, FUN, PERL, and WAN). The average cumulative distribution functions for the cryptocurrencies with the average inter-transaction time fulfilling the relations $\delta t < 1 \text{ s}$ (Group I, dotted red), $1 \text{ s} \leq \delta t < 2 \text{ s}$ (Group II, dotted blue), and $\delta t \geq 2 \text{ s}$ (Group III, dotted green) are also shown. Power laws with the scaling exponents γ and β assuming values typical for the financial markets— $\gamma = 3$ and $\beta = 3/2$ —are denoted by dashed lines. There is also a stretched exponential function fitted to the $v_{\Delta t}$ distributions for BTC and ETH on the right (black dotted line).

Another quantity that is frequently observed to be power-law-distributed is normalized volume traded in time unit $v_{\Delta t}(t_i) = (V_{\Delta t}(i) - \mu) / \sigma$ [16,23]:

$$P(X > v_{\Delta t}) \sim v_{\Delta t}^{-\beta}. \tag{2}$$

In this case, the exponent is much lower than for the absolute returns and corresponds to the Lévy-stable regime: $\beta < 2$. It was argued that there exists a simple relation between both the exponents: $\beta = \gamma/2$ [23]. Figure 2 (right panel) shows the cumulative distribution functions for $v_{\Delta t}$ for the same individual cryptocurrencies and their Groups I-III as in Figure 2 (left panel). Now, the cdfs for BTC and ETH do not develop power-law tails. A model that best fits them is the stretched exponential function $P(X > v_{\Delta t}) \sim \exp \sigma_v^{-\eta}$ with $\eta = 0.43$. However, in the case of less frequently traded cryptocurrencies, which belong to Group III, one can observe the power-law relation. What makes the results obtained here different from their counterparts for, for instance, the stock markets, is that one does not find any cryptocurrency with its cdf being a power law with the exponent $3/2$; the cdf tails decrease considerably faster here.

2.3. Price Impact

At this point, it is worthwhile to consider a possible causal relation between the returns and the volume despite the fact that no clear relation can be seen between their cdfs. It revokes the empirically well-documented observation that volume can influence price changes (both on the level of the order book and the level of the aggregated transaction volume), which is known in the literature as the price impact [21,23,65–68]. In order to investigate this issue, for each cryptocurrency, two parallel time series corresponding to $|R_{\Delta t}(t)|$ and $V_{\Delta t}(t)$ were input into the q -dependent detrended cross-correlation coefficient ρ_q measuring how correlated two detrended residual signals are across different scales [69]. The definition of the coefficient ρ_q , which allows one to quantify cross-correlations between two nonstationary signals, is based on the multifractal detrended cross-correlation analysis (MFCCA), whose algorithm can be sketched as follows [70].

In this particular case, there are two time series of length T and sampling intervals Δt : $|R_{\Delta t}(t_i)|$ and $V_{\Delta t}(t_i)$ with $i = 1, \dots, T$. One starts the procedure by dividing each time series into $M_s = 2 \lfloor T/s \rfloor$ non-overlapping segments of length s (called *scale*) going from both ends ($\lfloor \cdot \rfloor$ denotes the floor value). In each segment labelled by ν , both signals are integrated and polynomial trends $P_{\cdot, s, \nu}^{(m)}$ of degree m are removed:

$$\hat{R}_{\Delta t}(t_j, s, \nu) = \sum_{k=1}^j |R_{\Delta t}(t_{s(\nu-1)+k})| - P_{R, s, \nu}^{(m)}(t_j), \tag{3}$$

$$\hat{V}_{\Delta t}(t_j, s, \nu) = \sum_{k=1}^j V_{\Delta t}(t_{s(\nu-1)+k}) - P_{V, s, \nu}^{(m)}(t_j), \tag{4}$$

where $j = 1, \dots, s$ and $\nu = 1, \dots, M_s$. The detrended covariance is derived as

$$f_{|R|V}^2(s, \nu) = \frac{1}{s} \sum_{j=1}^s [\hat{R}_{\Delta t}(t_j, s, \nu) - \langle \hat{R}_{\Delta t}(t_j, s, \nu) \rangle_j] [\hat{V}_{\Delta t}(t_j, s, \nu) - \langle \hat{V}_{\Delta t}(t_j, s, \nu) \rangle_j], \tag{5}$$

where $\langle \cdot \rangle_j$ denotes the averaging over j . The detrended covariances calculated for all the segments ν are then used to determine the bivariate fluctuation function [70]:

$$F_q^{|R|V}(s) = \left\{ \frac{1}{M_s} \sum_{\nu=1}^{M_s} \text{sgn}[f_{|R|V}^2(s, \nu)] |f_{|R|V}^2(s, \nu)|^{q/2} \right\}^{1/q}. \tag{6}$$

Apart from the bivariate form given by the formula above, the univariate fluctuation functions $F_q^{|R||R|}(s)$ and $F_q^{VV}(s)$ can also be calculated but, in this case, the covariance functions become variances and do not need to be factorized into the sign and modulus parts as no negative value can occur.

The above elements of the formalism allow one to introduce the q -dependent detrended cross-correlation coefficient $\rho_q(s)$ defined as [69]:

$$\rho_q^{|R|V}(s) = \frac{F_q^{|R|V}(s)}{\sqrt{F_q^{|R||R|}(s) F_q^{VV}(s)}}. \tag{7}$$

By manipulating the value of the parameter q , one can focus on the correlations between fluctuations in different size: the large fluctuations $q > 2$ or the small fluctuations $q < 1$. For $q = 2$, all the fluctuations in time series are considered with the same weights. For positive q , values of ρ_q are restricted to the interval $[-1, 1]$, with their interpretation being similar to the interpretation of the classic Pearson coefficient C : $\rho_q = 1$ means a perfect correlation, $\rho_q = 0$ means independence, and $\rho_q = -1$ means a perfect anticorrelation. For negative q , the interpretation of the coefficient is more delicate and requires some experience [69]. Figure 3 presents the coefficient $\rho_q(s)$ calculated in a broad range of scales s for the selected individual cryptocurrencies (BTC, ETH, DOGE, FUN, PERL, and WAN) and the average $\rho_q(s)$ for Groups I-III. While different data sets are characterized by different strength of the detrended cross-correlations with Group I cross-correlated the strongest and Group 3 the weakest, there is an explicit division of scales into the short-scale range ($s < 1000$ min), where the correlations monotonously increase with increasing s , and the long-scale range ($s > 1000$ min), where one observes a kind of saturation-like behavior. In the latter, the correlations are characterized by $0.75 \leq \rho_q(s) \leq 0.95$, which means that the cryptocurrency market does not differ from other financial markets and its volatility $|R_{\Delta t}|$ and volume traded are strongly correlated. The two distinguished scale ranges are related to the information-processing speed of the market: it requires some amount of time for the investors to fully react to the incoming information and to build up the cross-correlations. One might view this result as a counterpart of the Epps effect for the detrended volatility–volume data [6,28,71–73]. The main difference between this market

and the regular financial markets is the relatively long cross-over scale ($s \approx 1000$ min), which can be associated with its worse liquidity.

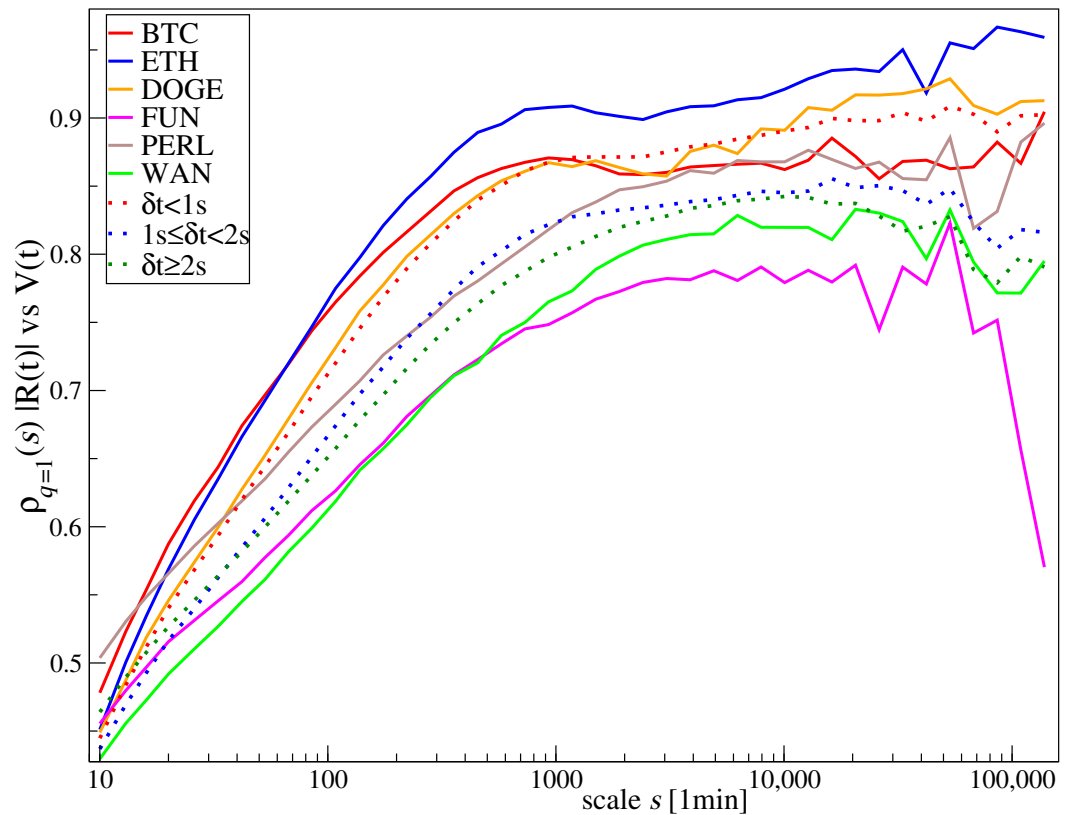


Figure 3. The q -dependent detrended cross-correlation coefficient $\rho_q(s)$ of order $q = 1$ calculated for volatility $|R_{\Delta t}(t)|$ and volume $V_{\Delta t}(t)$ (with $\Delta t = 1$ min) for the selected individual cryptocurrencies—BTC, ETH, DOGE, FUN, PERL, and WAN—where the cryptocurrency Groups I-III are characterized by a specific range of the average inter-transaction time: $\delta t < 1s$ (Group I, dotted red), $1s \leq \delta t < 2s$ (Group II, dotted blue), $\delta t \geq 2s$ (Group III, dotted green). The coefficient $\rho_q(s)$ has been averaged over all the cryptocurrencies belonging to a given group.

The next question to be asked is if there exists any functional relationship between $|R_{\Delta t}|$ and $V_{\Delta t}$. In order to address this question, $R_{\Delta t}$ vs. $V_{\Delta t}$ scatter plots for six selected cryptocurrencies were created; see Figure 4. In general, the cross-correlations identified by means of $\rho_q(s)$ can also be confirmed visually on these plots: the larger the volume, the larger the volatility can be. However, no specific functional form of $R_{\Delta t}(V_{\Delta t})$ can be inferred from this picture. Therefore, it is instructive to change the presentation to the conditional probability plots of the form $\mathbb{E}[f(|r_{\Delta t}|)|v_{\Delta t}]$, where the expectation value $\mathbb{E}[\cdot]$ can be approximated by the mean $\langle \cdot \rangle$. From the perspective of a market with substantially limited liquidity, small price changes correspond to small transaction volumes and constitute market noise. Thus, one may expect that the most interesting relation between volatility and volume can be seen for large returns: $|r_{\Delta t}(t)| \gg 1$.

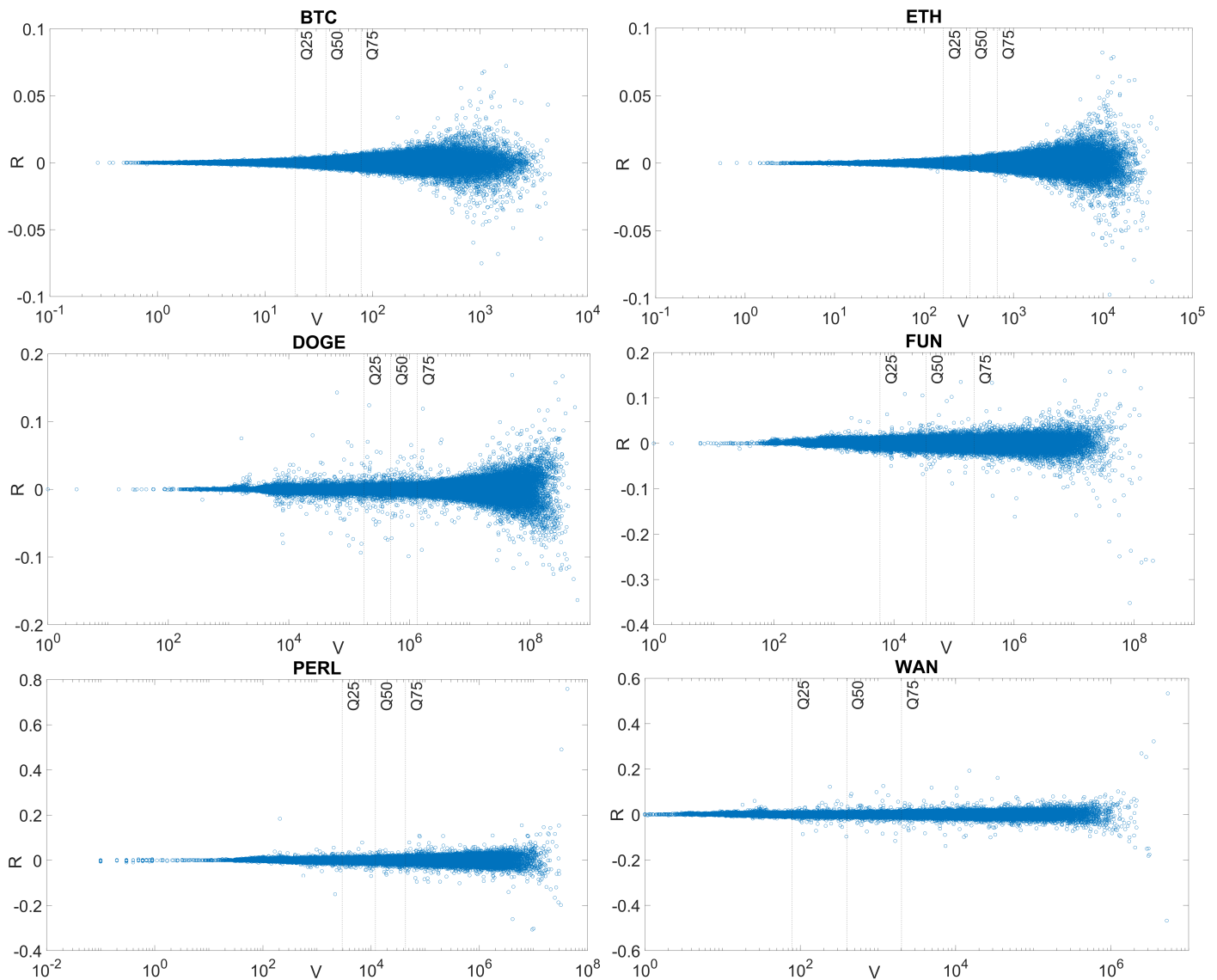


Figure 4. Scatter plots of the returns $R_{\Delta t}(t)$ and volume traded $V_{\Delta t}(t)$ for a few selected cryptocurrencies (BTC, ETH, DOGE, FUN, PERL, and WAN). Each point corresponds to a specific 1 min long interval in the whole 3-year-long period of interest. The vertical dashed lines in each panel denote the 25th, 50th, and 75th quantile of the volume probability distribution function for a given cryptocurrency. Note the logarithmic horizontal axis and the varying axis ranges among the panels.

The values of the normalized volume traded $v_{\Delta t}(t)$ were compartmentalized and, in each cell v_i , a fixed fraction $p \ll 1$ of the respective largest conditional volatility values was preserved for further analysis. A power-law function with the exponent κ is assumed to model a relation between the two quantities:

$$v_{\Delta t} \sim |r_{\Delta t}|^\kappa, \quad |r_{\Delta t}| \sim v_{\Delta t}^\alpha. \tag{8}$$

Figure 5 tests whether any of the relations of the form $\mathbb{E}[|r_{\Delta t}|^\kappa | v_{\Delta t}] \sim v_{\Delta t}$ hold for BTC if the following exponent values are selected: $\kappa = 0.2$, $\kappa = 0.5$, $\kappa = 1$, and $\kappa = 2$. The threshold value was chosen to be $p = 0.1$ because, for larger values, the relation becomes blurred and difficult to identify, whereas, for smaller values, too few data points can be considered, which amplifies the uncertainty. Looking at the graphs, one can reject the hypothesis that volatility and volume are related via $v_{\Delta t} \sim |r_{\Delta t}|^2$ (i.e., $\alpha = 0.5$) for all the sampling frequencies considered. In the case of the highest sampling frequency ($\Delta t = 1$ min), the data are approximated the best for $\kappa = 1$ and, secondarily, for $\kappa = 0.5$ and $\kappa = 0.2$, over the

broad volume range $1 < v_{\Delta t} < 16$. For $\Delta t \geq 10$ min, none of the values considered for κ work well, whereas, for $\Delta t = 5$ min, two cases cannot be excluded: $\kappa = 0.5$ and $\kappa = 0.2$. This means that the likely functional form of the price impact cannot be inferred based on the available data. Figure 6 presents the analogous results for ETH. The square-root form of the price impact (corresponding to $\kappa = 2$) can also be rejected in this case. However, it cannot be decided which of the remaining models ($\kappa \leq 1$) is the most likely.

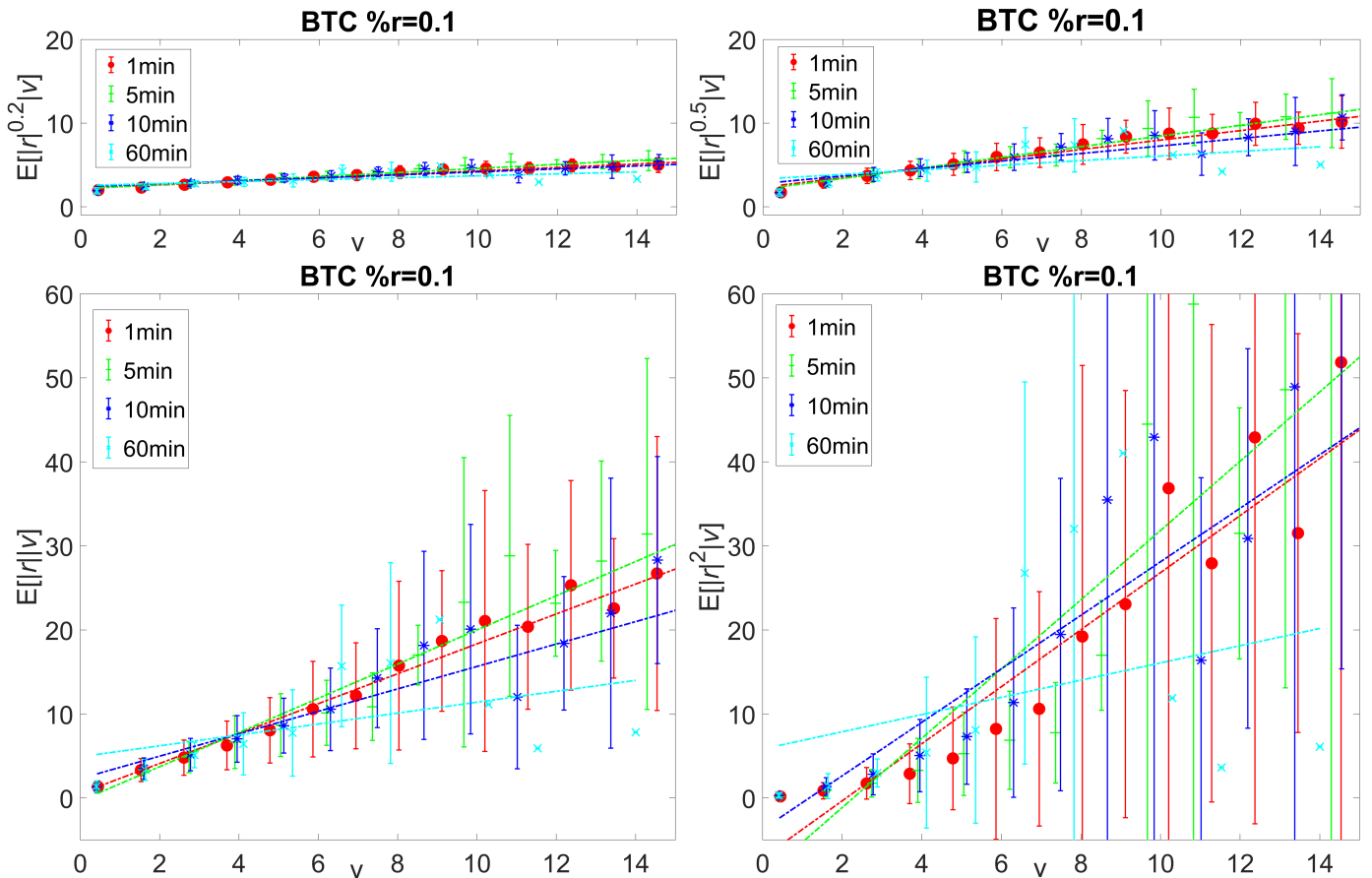


Figure 5. Conditional expectation $\mathbb{E}[|r_{\Delta t}|^\kappa | v_{\Delta t}]$ for BTC if only a p -fraction of the largest normalized returns $r_{\Delta t}$ is preserved for each value of the normalized volume $v_{\Delta t}$. Each panel shows the results for a specific value of κ together with a corresponding fitted power-law model. Four cases of the sampling interval are presented: $\Delta t = 1$ min, 5 min, 10 min, and 60 min. The error bars show the conditional standard deviation $\sigma[|r_{\Delta t}|^\kappa | v_{\Delta t}]$.

The fact that $\kappa \neq 2$ ($\alpha \neq 0.5$) and likely $\kappa \leq 1$ ($\alpha \geq 1$) for short sampling intervals is interesting because it makes the price impact function linear or superlinear ($\alpha \geq 1$): a result that differs from some earlier claims made for the regular financial markets, where the function was concave, at least for short and moderate sampling intervals [21,23]. There is also a discrepancy for the long sampling intervals because, in this case, the behavior reported for the regular markets was effectively linear, whereas here it remains undefined. It is noteworthy in this context that the superlinear ($\alpha > 1$) price impact for large Δt in Equation (8) could open the space for market manipulation [21], which, on the cryptocurrency trading platforms, can take the form of wash trading [18,74]. According to that, one can view the presented results as being in favor of the conclusion that full maturity is still ahead of the cryptocurrency market.

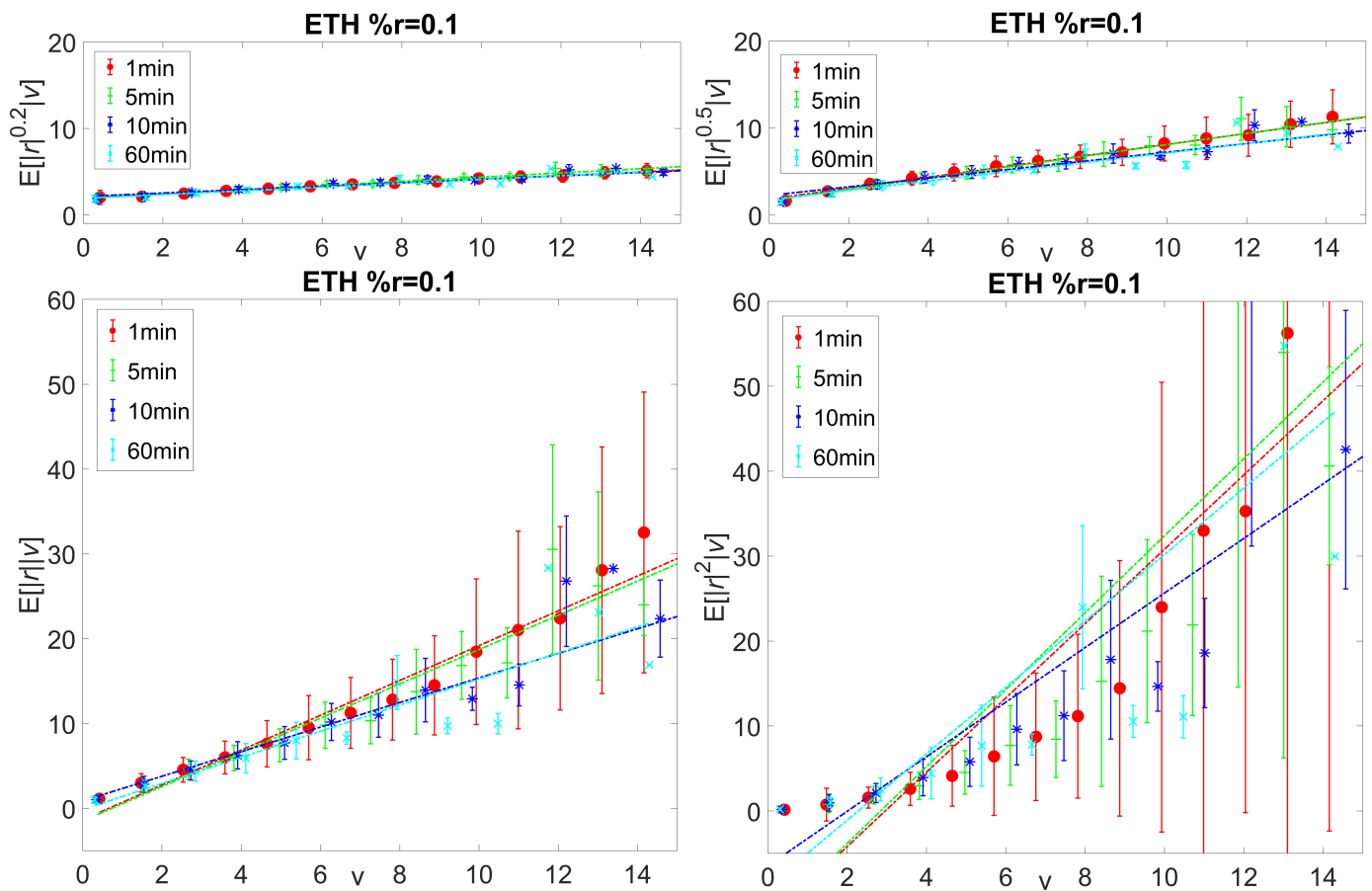


Figure 6. The same quantities as in Figure 5 for ETH.

2.4. Volatility Clustering and Long Memory

It takes some time for a market to completely absorb pieces of information that arrive there. This is a source of temporal market correlations that can be most easily observed in the price fluctuation amplitudes. Correlations are responsible for the phenomenon of volatility clustering, i.e., the existence of prolonged periods of fluctuations with elevated amplitude that are separated by quiet periods with more tamed fluctuations [75]. Volatility clustering is observed on all markets and can be quantified in terms of the autocorrelation function:

$$C(\tau) = \langle r_{\Delta t}(t)r_{\Delta t}(t - \tau) \rangle_t, \tag{9}$$

where τ is the lag time. The autocorrelation functions calculated from the absolute log-returns for several individual cryptocurrencies and the average autocorrelation functions calculated for Groups I–III are presented in Figure 7 on a double-logarithmic scale. In each case, one can identify at least one range of lags over which $C(\tau)$ shows power-law decay. For BTC, ETH, and FUN, there is only one such range corresponding to $10 \text{ min} \leq \tau \leq 500 \text{ min}$ with a relatively small upper end. The same refers to WAN but, in this case, the upper end exceeds $\tau \approx 20,000 \text{ min}$ (ca. two weeks). On the other hand, DOGE, PERL, and the average plots show two scaling regimes: the short- τ regime up to $\tau \approx 500\text{--}1000 \text{ min}$ (less than a day) and the long- τ regime for $1000 \text{ min} < \tau < 20,000 \text{ min}$. In each case, $C(\tau)$ falls to 0 around $\tau \approx 100,000 \text{ min}$ (more than 2 months). Compared to a more distant past, the scaling regions for BTC and ETH are shorter now (e.g., in the years 2016–2018, it reached $\tau = 1000 \text{ min}$ [29]), which is consistent with the market time acceleration caused by an increased trading frequency. This overall picture for the cryptocurrency market does not depart much from the one observed in other financial markets. A power-law decaying autocorrelation function expressing the long memory of volatility is a common property that is a manifestation of the way that the market processes

information [27,76]. The time lag at which $C(\tau)$ reaches a statistically insignificant level is equal to the average length of a volatility cluster [76]. Due to the alternating character of market dynamics, where the high-volatility periods are interwoven with low-volatility periods, for larger time lags, the autocorrelation function becomes negative. Note that, due to the fact that volatility time series are unsigned, the long-range autocorrelations cannot be exploited for the related investment strategies.

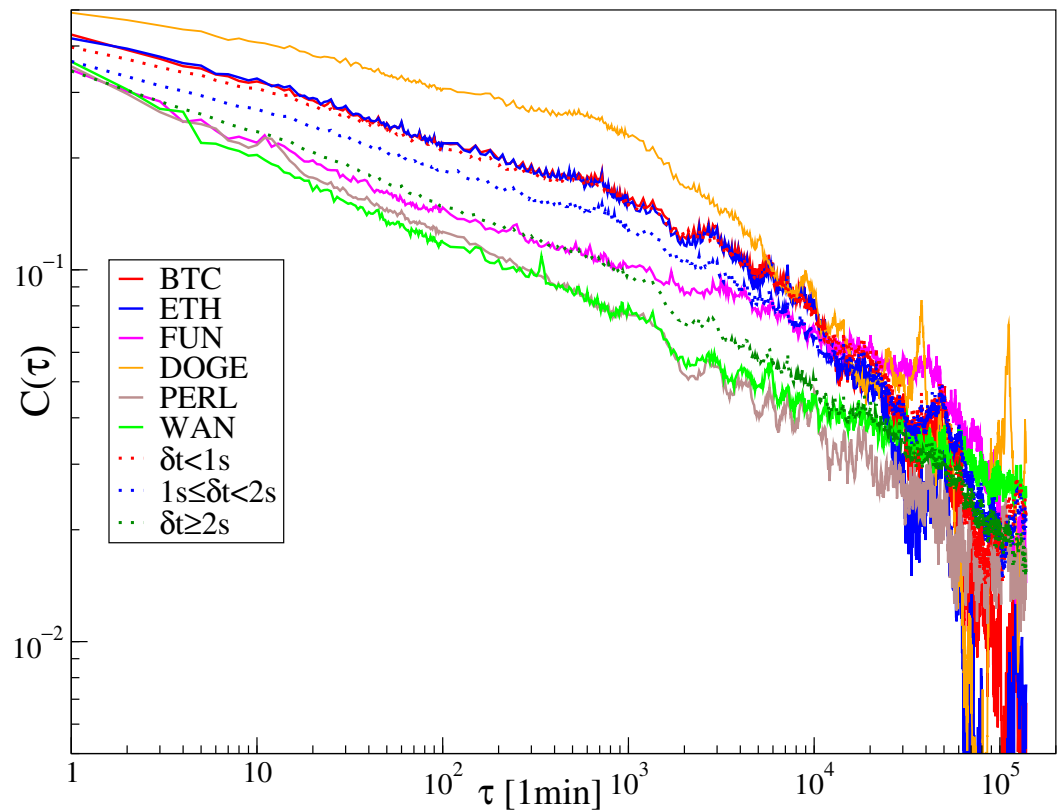


Figure 7. Autocorrelation function $C_{|r_{\Delta t}|}(\tau)$ of the absolute normalized log-returns $|r_{\Delta t}(t)|$ (volatility) calculated for the selected individual cryptocurrencies—BTC, ETH, DOGE, FUN, PERL, and WAN—as well as for the cryptocurrency Groups I-III characterized by specific range of the average inter-transaction time: $\delta t < 1s$ (Group I, dotted red), $1s \leq \delta t < 2s$ (Group II, dotted blue), $\delta t \geq 2s$ (Group III, dotted green). $C_{|r_{\Delta t}|}(\tau)$ has been averaged for each value of τ over all the cryptocurrencies belonging to a given group. Note the double-logarithmic scale.

2.5. Multiscaling of Returns

If the bivariate or univariate fluctuation functions can be approximated by a power-law relation

$$F_q^{AB}(s) \sim s^{h(q)}, \tag{10}$$

where $h(q)$ is a non-increasing function of q called the generalized Hurst exponent [77] and A and B stand for either R or V , the time series under study reveal a fractal structure. If $h(q) = \text{const} = H$, it means that this structure is monofractal, with H equal to the Hurst exponent, which is a measure of persistence; otherwise, it is multifractal [77]. Multifractal signals are governed by processes with long-range autocorrelations, which is why both properties are often observed together [78–81]. It is the case, for example, in financial data. If the relation (10) exists, it can be seen in double-logarithmic plots of $F_q^{AB}(s)$. Figure 8 displays $F_q^{RR}(s)$ for six cryptocurrencies, with $-4 \leq q \leq 4$ and $10 \leq s \leq 25,000$. Out of these, four cryptocurrencies show unquestionable power-law functions—BTC, ETH, DOGE, and FUN—for all used values of q and for at least a decade-long range of scales,

whereas PERL and WAN do not. The same result can be expressed in a different way by calculating the singularity spectra $f(\alpha)$ from $h(q)$ according to the following relations:

$$\alpha = h(q) + q \frac{dh(q)}{dq}, \quad f(\alpha) = q(\alpha - h(q)) + 1. \quad (11)$$

The Hölder exponents α quantify the singularity strength and $f(\alpha_0)$ expresses the fractal dimension of a subset of singularities with strength $\alpha = \alpha_0$. While many theoretical singularity spectra are symmetric, in a practical situation, one observes spectra that are asymmetric [14,28,31,82–85]. The insets in Figure 8 show $f(\alpha)$ calculated from $F_q^{RR}(s)$ in the scaling regions of s . All the presented spectra are left-side asymmetric (their left shoulder, corresponding to positive qs , is longer). The origin of such a behavior can be twofold: the signals can develop heavy tails of the probability distribution functions that are unstable in the sense of Lévy yet their convergence to the normal distribution is slow [76], and the signals can be mixtures of processes that have different fractal properties: large fluctuations can be associated with a multifractal process (e.g., a multiplicative cascade), whereas small fluctuations can be monofractal. It often happens that the small fluctuations in financial time series are noise whereas the medium and large fluctuations carry meaningful information.

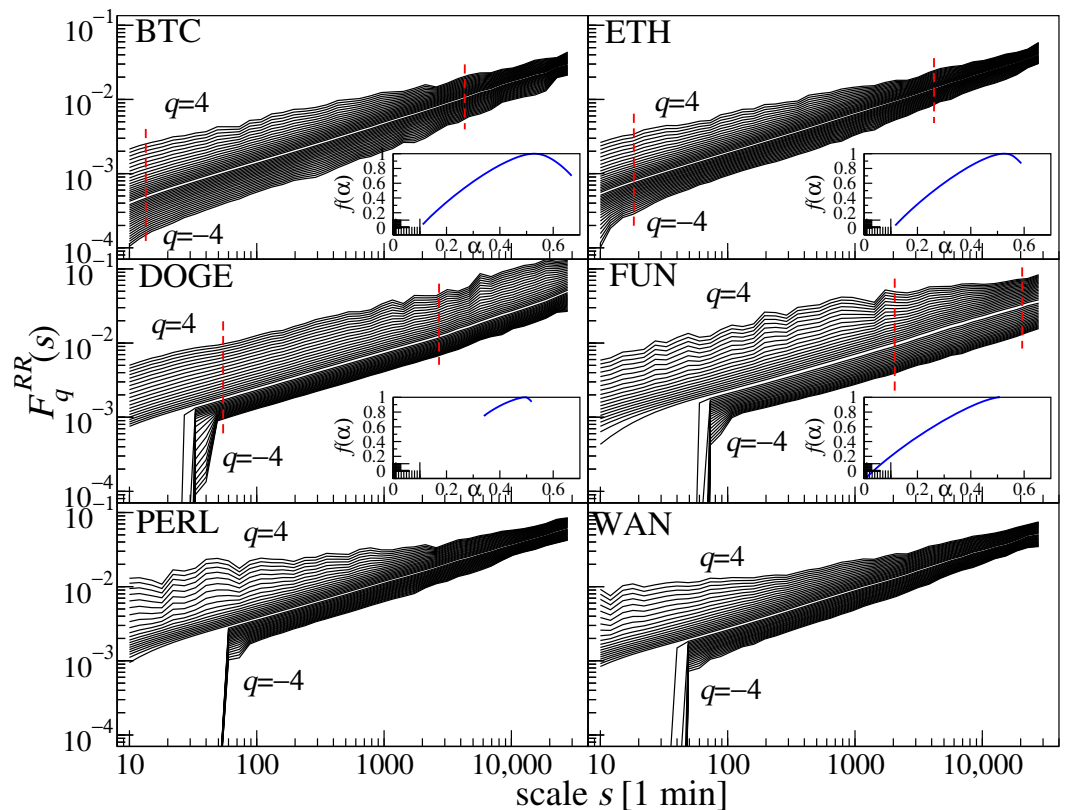


Figure 8. (Main plots) Univariate fluctuation functions $F_q^{RR}(s)$ calculated from the log-returns $R_{\Delta t}(t)$ with $\Delta t = 1$ min for BTC, ETH, DOGE, FUN, PERL, and WAN. The breakdown of scaling for small scales and negative values of q in some plots is an artifact related to long sequences of zero returns in time series. (Insets) Singularity spectra $f(\alpha)$ calculated from the corresponding fluctuation functions in the range denoted by dashed red lines (if possible).

It was reported in the literature that cryptocurrencies can also show such asymmetric $f(\alpha)$ spectra [6,14]. From the perspective of this study, it is interesting to note that the spectra for BTC calculated for different historical periods show an elongation of the right shoulder of $f(\alpha)$ that corresponds to small fluctuations. It can be interpreted as a gradual building of a multifractal structure in BTC price fluctuations that started from large returns only in the early stages of BTC trading and were imposed on the smaller returns as the

cryptocurrency market goes toward maturity. If one looks at Figure 8, BTC, ETH, and, to a lesser degree, DOGE—that is, the cryptocurrencies that are among the most capitalized ones—have noticeable right wings of $f(\alpha)$, whereas the more exotic cryptocurrencies, such as FUN, PERL, and WAN, do not develop the right wing at all. In agreement with what has been said before, despite various cryptoassets being traded on the same platforms, different ones can be found at different stages of the maturing process due to the different trading frequencies. This difference can also be observed in the possible scaling range of the fluctuation functions in Figure 8. In the case of the two most liquid cryptocurrencies, BTC and ETH, the $F_q^{RR}(s)$ scaling can be observed almost from the beginning of the scale range, whereas, in the case of less liquid cryptocurrencies, the range of satisfactory scaling is significantly shorter and $F_q^{RR}(s)$ even becomes singular on short scales due to the number of consecutive 1 min bins with zero returns. This is typical behavior in the case of less liquid financial instruments [14].

2.6. Cross-Correlations among Cryptocurrencies

Information that flows into the market may have the same impact on certain assets that, for example, share similar characteristics, such as the market sector, the main shareholders, or, in the case of cryptocurrency, the type or consensus mechanism [86]. This can lead to the emergence of cross-correlation between such assets and to a certain hierarchy of cross-correlations (e.g., sector, subsector, and bilateral ones) [87]. The correlation structure is a dynamical property that can change suddenly and substantially over time as the market reacts to perturbations [88]. In quiet times, it is well-shaped, elastic, and hierarchical, whereas, during periods of turmoil, it becomes centralized and rigid. This dual behavior is characteristic for the developed markets, while a lack of cross-correlations or a persistent centralization may be attributed to immaturity.

The market cross-correlation structure can be concisely characterized by the matrix approach. For a set of N time series of log-returns representing different cryptocurrencies $N(N - 1)/2$, the q -dependent detrended cross-correlation coefficients $\rho_q^{ij}(s)$ can be calculated, where $i, j = 1, \dots, N$ and $\rho_q^{ij} = \rho_q^{ji}$, which form a q -dependent detrended cross-correlation matrix $C_q(s)$. Due to the fact that the cross-correlation strength increases typically with scale for all the asset pairs, the differences in $\rho_q^{ij}(s)$ are, on average, minimal for the shortest studied scale of $s = 10$ min. However, even in this case, it is easy to observe that different cryptocurrency pairs reveal strong differences. Figure 9 presents the complete matrix $C_q(s)$ with the cryptocurrencies ordered according to the average inter-transaction time $\langle \delta t \rangle_t$. The ordering allows one to find even by eye a significant cross-correlation between $\langle \delta t \rangle_t$ and ρ_q^{ij} : the shorter this time is, the stronger the cross-correlations are. In full analogy to other markets, information needs time to propagate over the whole cryptocurrency market and the propagation speed is crucially dependent on the cryptocurrency liquidity, which can roughly be approximated by the transaction number per time unit. Based on the exact values of $\rho_q^{ij}(s)$, one can notice that even the least frequently traded cryptocurrencies from the considered basket develop statistically significant dependencies among themselves. This, however, might not be true for even less capitalized tokens, which can have idiosyncratic dynamics.

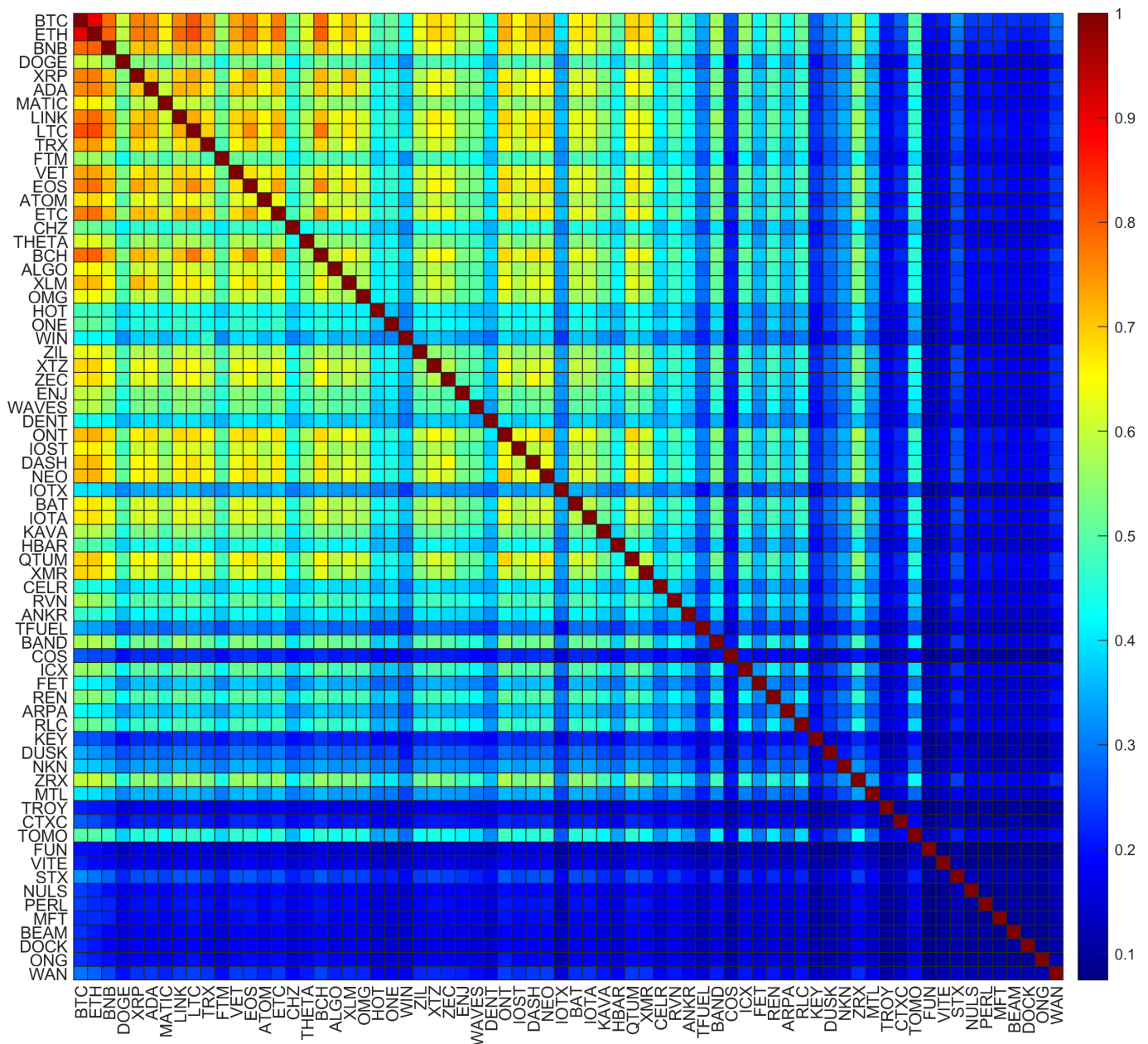


Figure 9. The q -dependent detrended cross-correlation matrix entries $\rho_q^{ij}(s)$ calculated from time series of log-returns representing 70 cryptocurrencies with $q = 1$ and $s = 10$ min. Cryptocurrencies have been sorted according to the average inter-transaction time δt in increasing order (top to bottom). The color-coding scheme is shown on the right.

The correlation matrix $\mathbf{C}_q(s)$ can be transformed into a distance matrix $\mathbf{D}_q(s)$ with the entries

$$d_q^{ij}(s) = \sqrt{2(1 - \rho_q^{ij}(s))}, \quad (12)$$

which differs from the former in that its entries $d_q^{(ij)}$ are metric. $\mathbf{D}_q(s)$ can be used for constructing a weighted graph with nodes representing cryptocurrencies and edges representing distances $d_q^{(ij)}(s)$. Next, by using the Prim algorithm [89], one can construct the corresponding q -dependent detrended minimal spanning tree (MST), which can be considered as a connected minimum-weight subset of the graph containing all N nodes and $N - 1$ edges. The MST topology depends strongly on the cross-correlation structure of a market. A centralized market corresponds to a star-like MST, whereas a market contain-

ing idiosyncratic assets shows an MST with elongated branches and no dominant hubs. Figure 10 exhibits two MSTs created from all 70 cryptocurrencies for $q = 1$ (left) and $q = 4$ (right). The former involves cross-correlations between the fluctuations in all magnitudes, whereas the latter involves only the large fluctuations. For $q = 1$, the structure is dual-star with BTC and ETH as its central hubs. This is not surprising as both cryptocurrencies are distinguished by their fame and large capitalization, which makes them a kind of reference for the remaining cryptocurrencies. On the other hand, for $q = 4$, the structure is more distributed, with a primary hub, BTC, and a few secondary ones: LTC, XMR, and ONT. This means that the relatively large fluctuations are not collectively correlated, unlike the majority of fluctuations, and more subtle dependencies are present. This is in parallel with the conclusions based on the multifractal analysis, which were large fluctuations that carried clearly multifractal characteristics and long-term correlations, whereas the small fluctuations were much more noisy. It is worth mentioning that a similar behavior can be observed in the stock market, where the cross-correlation structure carried by the large fluctuations is much richer than that carried by the medium and small fluctuations [90]. However, in the stock market, the heterogeneous cross-correlation structure is more pronounced even in the latter case [86,90]. Since there is no clear division into market sectors [91], the cryptocurrency market appears to be less developed from this particular perspective.

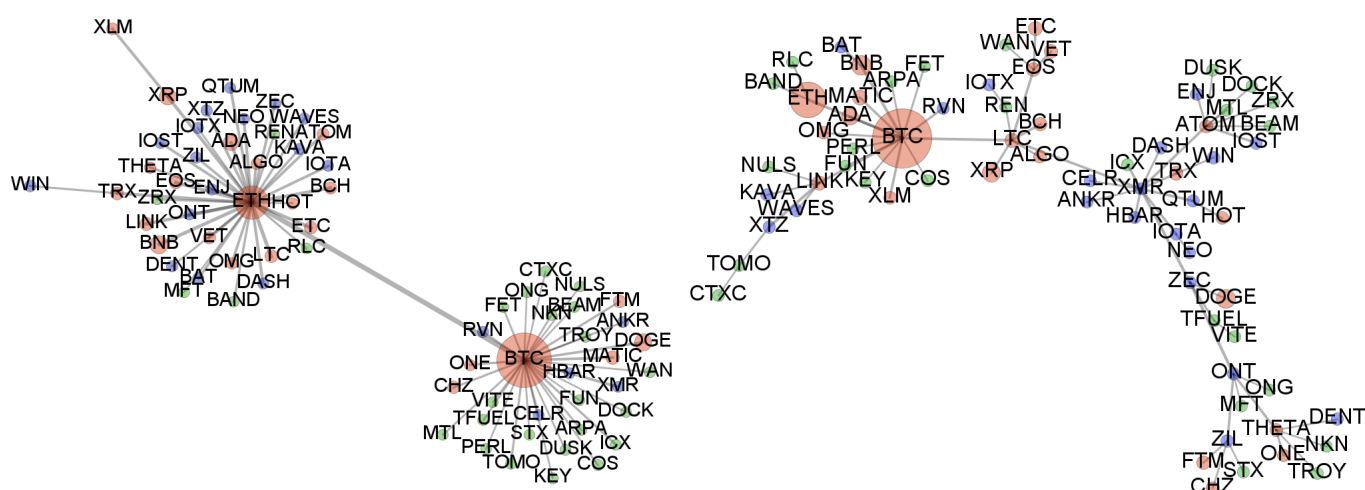


Figure 10. Minimal spanning trees calculated from a distance matrix $D_q(s)$ based on $\rho_q(s)$ for $s = 10$ and for $q = 1$ (left) and $q = 4$ (right). Within each tree, the size of the vertex is proportional to the average value of the volume $W_{\Delta t}$ for $\Delta t = 1$ min, while the width of the edge is proportional to $1 - d_q^H(s)$. The vertex sizes cannot be directly compared across the trees, however. Colors represent Groups I-III in terms of the trading frequency: $\delta t < 1s$ (Group I, red), $1s \leq \delta t < 2s$ (Group II, blue), and $\delta t \geq 2s$ (Group III, green).

2.7. Cross-Correlations between Cryptocurrencies and Other Markets

Recently, BTC and ETH have been found to be significantly coupled to the traditional financial markets during the period covering the COVID-19 pandemic and the bear market of 2022 [55]. This result has essential practical implications in risk management as cryptocurrencies cannot serve as hedging assets [92]. It differs from earlier findings that, before 2020, the cryptocurrency market was detached from the traditional markets [47,52,93,94], but, at the same time, it remains in agreement with the observations that COVID-19 changed the safe-haven paradigm and contributed to the correlation of major cryptocurrencies with traditional risk assets [53,95–98]. So far, only the most capitalized cryptocurrencies have been studied [55], and this is why cryptocurrencies with smaller capitalization were also studied here.

The time series of log-returns of 70 cryptocurrencies and 22 traditional financial instruments were collected from Dukascopy platform [99]. Among the latter, there are

contracts for difference (CFDs) representing the returns of 12 fiat currencies (AUD, CAD, CHF, CNH, EUR, GBP, JPY, MXN, NOK, NZD, PLN, and ZAR), 4 commodities (WTI crude oil (CL), high-grade copper (HG), silver (XAG), and gold (XAU)), 4 US stock market indices (Nasdaq 100 (NQ100), S&P500, Down Jones Industrial Average (DJI), and Russell 2000 (RUSSEL)), the main German stock index DAX 40 (DAX), and the Japanese Nikkei 225 (NIKKEI). All these instruments except for the non-US stock indices were expressed in USD. Their quotes cover a period from 1 January 2020 to 30 December 2022. The quotes were recorded over the trading hours, i.e., from Sunday 22:00 to Friday 20:15 UTC, with a break between 20:15 and 22:00 UTC each trading day. In order to assess the cross-correlations, the cryptocurrency time series were synchronized with those from Dukascopy. Cross-correlations were quantified by $\rho_q^{RR}(s)$.

Figure 11 shows the q -dependent detrended cross-correlation matrix $C_q(s)$ entries for the inter-market pairs consisting of a cryptocurrency and a traditional asset. The first observation is that the maximum available values of the matrix entries do not exceed $\rho_q^{RR}(s) = 0.25$, which makes them much smaller than in the case of the inner cross-correlation among the cryptocurrencies. This is an expected effect because markets are typically more tightly coupled inside than outside. Among the strongest cross-correlations, one can point out the coupling of BTC and ETH with the American stock market indices ($\rho_q^{RR}(s) > 0.2$ and with NIKKEI and DAX ($0.15 < \rho_q^{RR}(s) < 0.2$). Considerably weaker yet still prominent are the cross-correlations between several other cryptocurrencies, such as XRP, ADA, LTC, LINK, VET, ETC, EOS, ATOM, and BCH on one side and the American indices ($0.15 < \rho_q^{RR}(s) < 0.2$). The relations between cryptocurrencies and fiat currencies remain moderate, with the AUD, CAD, and NZD being the relatively strongest ($0.1 < \rho_q^{RR}(s) < 0.15$). Contrary to this, the cryptocurrencies are the most decoupled from JPY, CHF, gold (XAU), and crude oil (CL). A general observation is that the less liquid a cryptocurrency is, the weaker its cross-correlation with traditional instruments. Here again, DOGE is somewhat of an exception and has a weaker cross-correlation than its trading frequency and capitalization would imply. However, it should be noted that the values collected in Figure 11 correspond to the shortest available scale of $s = 10$ min. How these values refer to the maximum cross-correlations for longer scales is documented in Figure 12. Here, the cross-correlation between the selected cryptocurrencies and their sets grouped according to the average inter-transaction time (Groups I–III) and NASDAQ 100 is presented. This particular choice of the traditional index was motivated by the fact that the cryptocurrency market is strongly cross-correlated with it [55]. Indeed, for much longer s , the values of $\rho_q^{RR}(s)$ grow significantly and even reach some saturation level resembling the Epps effect for $s > 500$ min, with the average values of $\rho_q^{RR}(s)$ in Groups I–III oscillating around 0.4 (for a given scale, $\rho_q^{RR}(s)$ decreases systematically with an increasing δt). The cryptocurrencies that are the most cross-correlated with NASDAQ 100, i.e., BTC and ETH, have maximum values of $\rho_q^{RR}(s) > 0.5$.

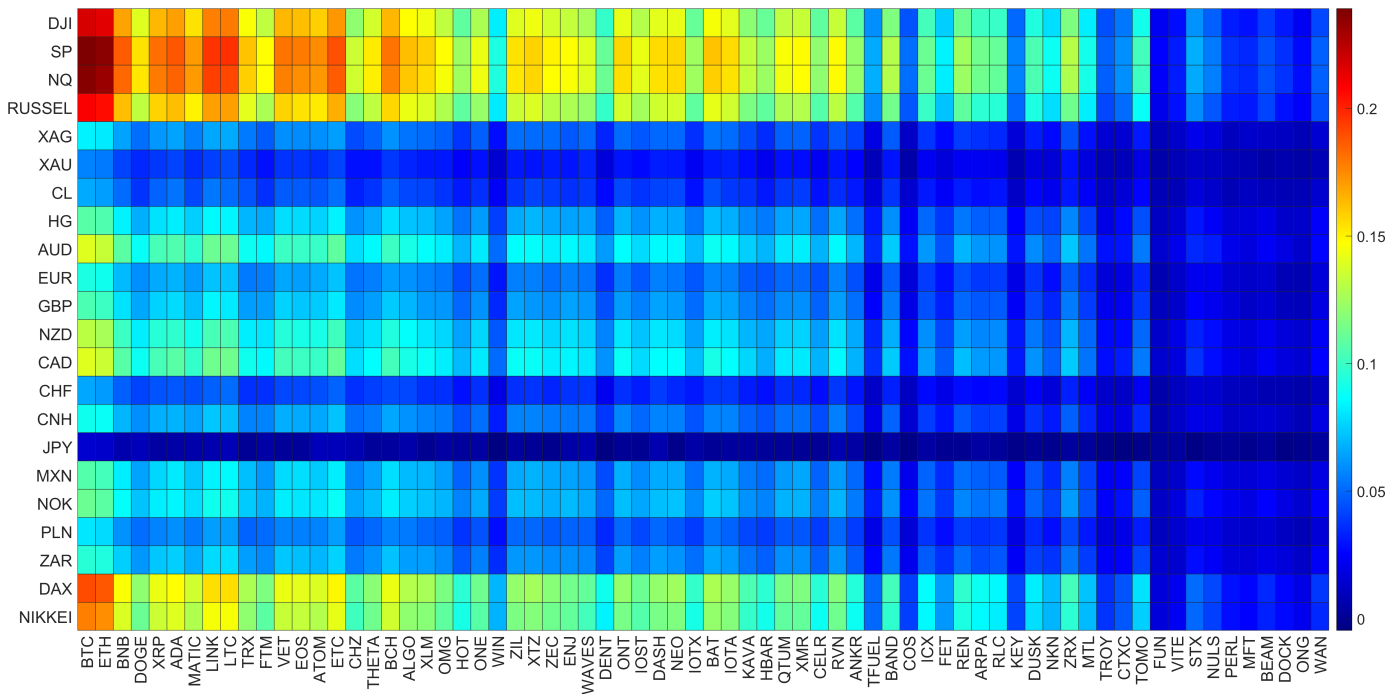


Figure 11. The q -dependent detrended cross-correlation matrix entries $\rho_q^{ij}(s)$ calculated from time series of log-returns representing selected cryptocurrencies and selected traditional financial instruments with $q = 1$ and $s = 10$ min. Cryptocurrencies have been sorted according to the average inter-transaction time δt in increasing order (top to bottom). The color coding scheme, which differs from the one in Figure 9, is shown on the right.

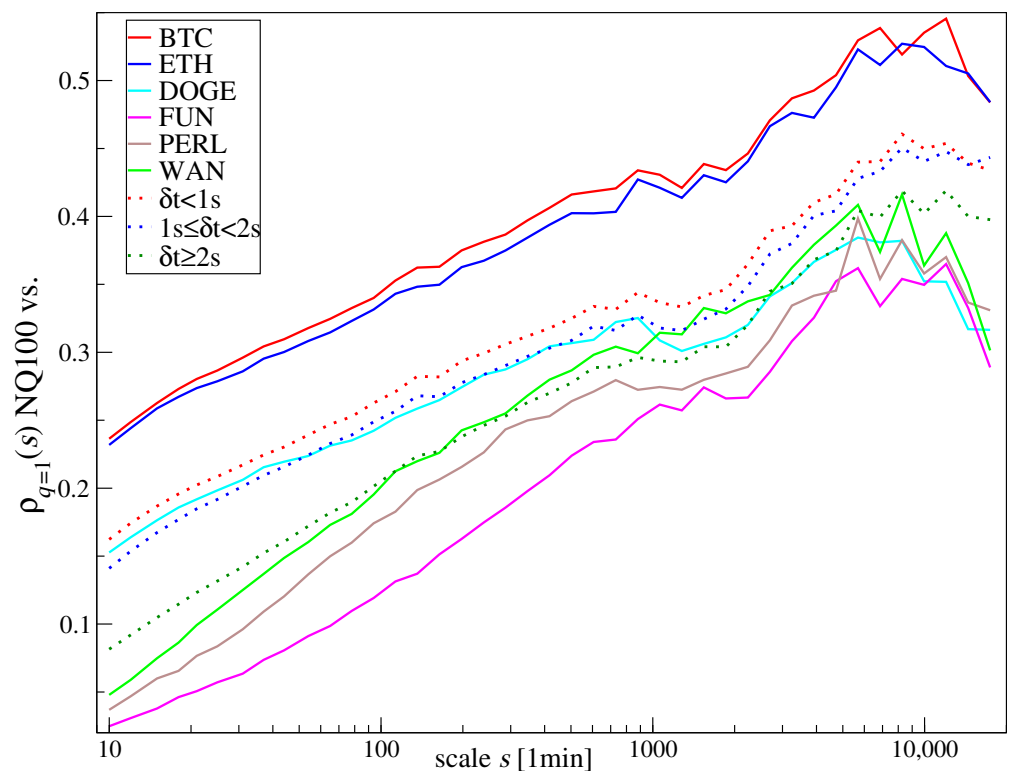


Figure 12. The q -dependent detrended cross-correlation coefficient $\rho_q^{RR}(s)$ calculated for the pairs of log-return time series consisting of NASDAQ 100 and a cryptocurrency (BTC, ETH, DOGE, FUN, PERL, or WAN) or a group of cryptocurrencies characterized by average inter-transaction time from a specific range: $\delta t < 1s$ (Group I, red), $1s \leq \delta t < 2s$ (Group II, blue), and $\delta t \geq 2s$ (Group III, green).

3. Conclusions

The statistical properties of price log-returns and the volume of the cryptocurrencies were the central points of the present study. The existence of the so-called financial stylized facts in the cryptocurrency market during the last 3 years was investigated and compared with the stylized facts observed in the traditional financial markets. Several characteristics were of particular interest: a tail behavior of the probability distribution functions for the log-returns and volume traded, the functional form of price impact, volatility autocorrelations, multiscaling, cross-correlations among the cryptocurrencies, and cross-correlations between the principal cryptocurrencies and selected traditional market assets. Almost all the analyzed characteristics of the cryptocurrency market were found to be in qualitative agreement with their counterparts from the traditional markets. It allows one to conclude that, from this particular perspective, the cryptocurrency market does not differ from the mature markets.

Despite such a positive conclusion, one still has to be cautious. First, the level of the maturity of the cryptocurrencies depends on their trading frequency. The most liquid ones, such as BTC and ETH, to a greater extent, have characteristics corresponding to mature financial markets, and the least liquid ones do not. Second, the price impact function, while also of a power-law form, results in being substantially different from its counterparts reported in the traditional markets (linear or convex here vs. concave there [21]). Third, while the statistical properties are important from a practical point of view as they can be exploited in various investment strategies, there are nevertheless many other important indicators of market maturity that were not investigated here. For example, the number of cryptocurrencies traded on the largest platforms, such as Binance, is so large that it already matches the world's largest markets, such as the New York Stock Exchange and NASDAQ. On the other hand, even the most recognized cryptocurrencies, such as BTC and ETH, show extreme volatility, which means that the market is still rather illiquid, and this property can question its maturity. There is another problem associated with the fact that the cryptocurrencies are often viewed as speculation toys rather than full-scale investment instruments. There are also numerous issues related to the limited reliability of the cryptocurrencies, their weak supply elasticity, etc. These problems, while important, were beyond the scope of this analysis, which one has to keep in mind when thinking about the given conclusions. Repeating this kind of analysis in future in order to follow how the cryptocurrency market changes seems to be a straightforward direction of potential future studies.

Author Contributions: Individual contributions of the authors are as follows. Conceptualization, S.D. and M.W.; methodology, S.D., J.K. and M.W.; software, M.W.; validation, S.D., J.K. and M.W.; formal analysis, S.D. and M.W.; investigation, S.D., J.K. and M.W.; resources, M.W.; data curation, M.W.; writing—original draft preparation, J.K.; writing—review and editing, S.D., J.K. and M.W.; visualization, M.W.; supervision, S.D. and J.K.; project administration, S.D. and M.W. All authors have read and agreed to the published version of the manuscript.

Funding: This research received no external funding.

Data Availability Statement: The data used in the article are freely available on Binance and Dukascopy platforms.

Conflicts of Interest: The authors declare no conflict of interest.

Appendix A

Table A1. List of cryptocurrencies from Binance.

Ticker	Name	Ticker	Name	Ticker	Name
ADA	cardano	FET	fetch	QTUM	qtum
ALGO	algorand	FTM	fantom	REN	ren
ANKR	ankr	FUN	funtoken	RLC	iexec
ARPA	arpa chain	HBAR	hedera	RVN	ravencoin
ATOM	cosmos	HOT	holo	STX	stacks
BAND	band protocol	ICX	icon	TFUEL	theta fuel
BAT	basic attention token	IOST	iost	THETA	theta
BCH	bitcoin cash	IOTA	miota	TOMO	tomochain
BEAM	beam	IOTX	iotex	TROY	troy
BNB	binance coin	KAVA	kava	TRX	tron
BTC	bitcoin	KEY	key	VET	vechain
CELR	celer network	LINK	chainlink	VITE	vite
CHZ	chiliz	LTC	litecoin	WAN	wanchain
COS	contentos	MATIC	polygon	WAVES	waves
CTXC	cortex	MFT	hifi finance	WIN	winklink
DASH	dash	MTL	metal	XLM	stellar
DENT	dent	NEO	neo	XMR	monero
DOCK	dock	NKN	nkn	XRP	ripple
DOGE	dogecoin	NULS	nuls	XTZ	tezos
DUSK	dusk network	OMG	omg network	ZEC	zcash
ENJ	enj coin	ONE	harmony	ZIL	zilliqa
EOS	eos	ONG	ontology gas	ZRX	0x
ETC	ethereum classic	ONT	ontology		
ETH	ethereum	PERL	perl		

References

- Wattenhofer, R. *The Science of the Blockchain*; CreateSpace Independent Publishing Platform: Scotts Valley, CA, USA, 2016.
- Lantz, L.; Cawrey, D. *Mastering Blockchain*; O'Reilly Media: Sebastopol, CA, USA, 2020.
- Corbet, S.; Lucey, B.; Urquhart, A.; Yarovaya, L. Cryptocurrencies as a financial asset: A systematic analysis. *Int. Rev. Financ. Anal.* **2019**, *62*, 182–199. [[CrossRef](#)]
- Gil-Cordero, E.; Cabrera-Sánchez, J.P.; Arrás-Cortés, M.J. Cryptocurrencies as a financial tool: Acceptance factors. *Mathematics* **2020**, *8*, 1974. [[CrossRef](#)]
- Cachanosky, N. Can cryptocurrencies become a commonly accepted means of exchange? In *The Economics of Blockchain and Cryptocurrency AIER Sound Money Project*; Working Paper No. 2020-14; Edward Elgar Publishing: Cheltenham, UK, 2020.
- Wątorek, M.; Drożdż, S.; Kwapien, J.; Minati, L.; Oświęcimka, P.; Stanuszek, M. Multiscale characteristics of the emerging global cryptocurrency market. *Phys. Rep.* **2021**, *901*, 1–82. [[CrossRef](#)]
- James, N.; Menzies, M. Collective correlations, dynamics, and behavioural inconsistencies of the cryptocurrency market over time. *Nonlinear Dyn.* **2022**, *107*, 4001–4017. [[CrossRef](#)] [[PubMed](#)]
- Ausloos, M. Statistical physics in foreign exchange currency and stock markets. *Physica A* **2000**, *285*, 48–65. [[CrossRef](#)]
- Cont, R. Empirical properties of asset returns: Stylized facts and statistical issues. *Quant. Financ.* **2001**, *1*, 223–236. [[CrossRef](#)]
- LeBaron, B. Agent-based financial markets: Matching stylized facts with style. In *Post Walrasian Macroeconomics: Beyond the Dynamic Stochastic General Equilibrium Model*; Cambridge University Press: Cambridge, UK, 2006; pp. 221–236.
- Morone, A. Financial markets in the laboratory: An experimental analysis of some stylized facts. *Quant. Financ.* **2008**, *8*, 513–532. [[CrossRef](#)]

12. Wątopek, M.; Kwapien, J.; Drożdż, S. Financial return distributions: Past, present, and COVID-19. *Entropy* **2021**, *23*, 884. [[CrossRef](#)]
13. Begušić, S.; Kostanjčar, Z.; Eugene Stanley, H.; Podobnik, B. Scaling properties of extreme price fluctuations in Bitcoin markets. *Physica A* **2018**, *510*, 400–406. [[CrossRef](#)]
14. Drożdż, S.; Gębarowski, R.; Minati, L.; Oświęcimka, P.; Wątopek, M. Bitcoin market route to maturity? Evidence from return fluctuations, temporal correlations and multiscaling effects. *Chaos* **2018**, *28*, 071101. [[CrossRef](#)]
15. Pessa, A.A.; Perc, M.; Ribeiro, H.V. Age and market capitalization drive large price variations of cryptocurrencies. *Sci. Rep.* **2023**, *13*, 3351. [[CrossRef](#)] [[PubMed](#)]
16. Gopikrishnan, P.; Plerou, V.; Gabaix, X.; Stanley, H.E. Statistical properties of share volume traded in financial markets. *Phys. Rev. E* **2000**, *62*, R4493. [[CrossRef](#)] [[PubMed](#)]
17. Plerou, V.; Stanley, H.E.; Gabaix, X.; Gopikrishnan, P. On the origin of power-law fluctuations in stock prices. *Quant. Financ.* **2004**, *4*, 11–15. [[CrossRef](#)]
18. Kwapien, J.; Wątopek, M.; Bezbradica, M.; Crane, M.; Tan Mai, T.; Drożdż, S. Analysis of inter-transaction time fluctuations in the cryptocurrency market. *Chaos* **2022**, *32*, 083142. [[CrossRef](#)]
19. Navarro, R.M.; Leyvraz, F.; Larralde, H. Statistical properties of volume in the Bitcoin/USD market. *arXiv Prepr.* **2023**, arXiv:2304.01907.
20. Gillemot, L.; Farmer, J.D.; Lillo, F. There's more to volatility than volume. *Quant. Financ.* **2006**, *6*, 371–384. [[CrossRef](#)]
21. Bouchaud, J.P. Price impact. In *Encyclopedia of Quantitative Finance*; Cambridge University Press: Cambridge, UK, 2010; pp. 1–6.
22. Tóth, B.; Lempérière, Y.; Deremble, C.; Lataillade, J.D.; Kockelkoren, J.; Bouchaud, J.P. Anomalous price impact and the critical nature of liquidity in financial markets. *Phys. Rev. X* **2011**, *1*, 021006.
23. Gabaix, X.; Gopikrishnan, P.; Plerou, V.; Stanley, H.E. A theory of power-law distributions in financial market fluctuations. *Nature* **2003**, *423*, 267–270. [[CrossRef](#)]
24. Rak, R.; Drożdż, S.; Kwapien, J.; Oświęcimka, P. Stock returns versus trading volume: Is the correspondence more general? *Acta Phys. Pol. B* **2013**, *44*, 2035–2050. [[CrossRef](#)]
25. Bucci, F.; Benzaquen, M.; Lillo, F.; Bouchaud, J.P. Crossover from linear to square-root market impact. *Phys. Rev. Lett.* **2019**, *122*, 108302. [[CrossRef](#)]
26. Zarinelli, E.; Treccani, M.; Farmer, J.D.; Lillo, F. Beyond the square root: Evidence for logarithmic dependence of market impact on size and participation rate. *Mark. Microstruct. Liq.* **2015**, *1*, 1550004. [[CrossRef](#)]
27. Gopikrishnan, P.; Plerou, V.; Nunes Amaral, L.A.; Meyer, M.; Stanley, H.E. Scaling of the distribution of fluctuations of financial market indices. *Phys. Rev. E* **1999**, *60*, 5305–5316. [[CrossRef](#)] [[PubMed](#)]
28. Drożdż, S.; Kwapien, J.; Oświęcimka, P.; Rak, R. The foreign exchange market: Return distributions, multifractality, anomalous multifractality and the Epps effect. *New J. Phys.* **2010**, *12*, 105003. [[CrossRef](#)]
29. Drożdż, S.; Minati, L.; Oświęcimka, P.; Stanuszek, M.; Wątopek, M. Signatures of the crypto-currency market decoupling from the Forex. *Future Internet* **2019**, *11*, 154. [[CrossRef](#)]
30. Matia, K.; Ashkenazy, Y.; Stanley, H.E. Multifractal properties of price fluctuations of stocks and commodities. *Europhys. Lett.* **2003**, *61*, 422–428. [[CrossRef](#)]
31. Kwapien, J.; Oświęcimka, P.; Drożdż, S. Components of multifractality in high-frequency stock returns. *Physica A* **2005**, *350*, 466–474. [[CrossRef](#)]
32. Oświęcimka, P.; Kwapien, J.; Drożdż, S. Multifractality in the stock market: Price increments versus waiting times. *Physica A* **2005**, *347*, 626–638. [[CrossRef](#)]
33. Takaishi, T. Statistical properties and multifractality of Bitcoin. *Physica A* **2018**, *506*, 507–519. [[CrossRef](#)]
34. Kristjanpoller, W.; Bouri, E. Asymmetric multifractal cross-correlations between the main world currencies and the main cryptocurrencies. *Physica A* **2019**, *523*, 1057–1071. [[CrossRef](#)]
35. Han, Q.; Wu, J.; Zheng, Z. Long-range dependence, multi-fractality and volume-return causality of ether market. *Chaos: Interdiscip. J. Nonlinear Sci.* **2020**, *30*, 011101. [[CrossRef](#)]
36. Takaishi, T.; Adachi, T. Market efficiency, liquidity, and multifractality of Bitcoin: A dynamic study. *Asia-Pac. Financ. Mark.* **2020**, *27*, 145–154. [[CrossRef](#)]
37. Bariviera, A.F. One model is not enough: Heterogeneity in cryptocurrencies' multifractal profiles. *Financ. Res. Lett.* **2021**, *39*, 101649. [[CrossRef](#)]
38. Takaishi, T. Time-varying properties of asymmetric volatility and multifractality in Bitcoin. *PLoS ONE* **2021**, *16*, e0246209. [[CrossRef](#)] [[PubMed](#)]
39. Kakinaka, S.; Umeno, K. Asymmetric volatility dynamics in cryptocurrency markets on multi-time scales. *Res. Int. Bus. Financ.* **2022**, *62*, 101754. [[CrossRef](#)]
40. Wątopek, M.; Kwapien, J.; Drożdż, S. Multifractal cross-correlations of bitcoin and ether trading characteristics in the post-COVID-19 time. *Future Internet* **2022**, *14*, 215. [[CrossRef](#)]
41. Drożdż, S.; Gruemmer, F.; Ruf, F.; Speth, J. Towards identifying the world stock market cross-correlations: DAX versus Dow Jones. *Physica A* **2001**, *294*, 226–234. [[CrossRef](#)]
42. Plerou, V.; Gopikrishnan, P.; Rosenow, B.; Amaral, L.A.N.; Guhr, T.; Stanley, H.E. Random matrix approach to cross correlations in financial data. *Phys. Rev. E* **2002**, *65*, 066126. [[CrossRef](#)]

43. Maslov, S. Measures of globalization based on cross-correlations of world financial indices. *Physica A* **2001**, *301*, 397–406. [[CrossRef](#)]
44. Nguyen, A.P.N.; Mai, T.T.; Bezbradica, M.; Crane, M. The Cryptocurrency Market in Transition before and after COVID-19: An Opportunity for Investors? *Entropy* **2022**, *24*, 1317. [[CrossRef](#)]
45. James, N.; Menzies, M.; Chin, K. Economic state classification and portfolio optimisation with application to stagflationary environments. *Chaos Solitons Fractals* **2022**, *164*, 112664. [[CrossRef](#)]
46. James, N.; Menzies, M.; Chan, J. Semi-metric portfolio optimization: A new algorithm reducing simultaneous asset shocks. *Econometrics* **2023**, *11*, 8. [[CrossRef](#)]
47. Corbet, S.; Meegan, A.; Larkin, C.; Lucey, B.; Yarovaya, L. Exploring the dynamic relationships between cryptocurrencies and other financial assets. *Econ. Lett.* **2018**, *165*, 28–34. [[CrossRef](#)]
48. Wang, P.; Zhang, W.; Li, X.; Shen, D. Is cryptocurrency a hedge or a safe haven for international indices? A comprehensive and dynamic perspective. *Financ. Res. Lett.* **2019**, *31*, 1–18. [[CrossRef](#)]
49. Shahzad, S.J.H.; Bouri, E.; Roubaud, D.; Kristoufek, L.; Lucey, B. Is Bitcoin a better safe-haven investment than gold and commodities? *Int. Rev. Financ. Anal.* **2019**, *63*, 322–330. [[CrossRef](#)]
50. Shahzad, S.J.H.; Bouri, E.; Roubaud, D.; Kristoufek, L. Safe haven, hedge and diversification for G7 stock markets: Gold versus bitcoin. *Econ. Model.* **2020**, *87*, 212–224. [[CrossRef](#)]
51. Bouri, E.; Shahzad, S.J.H.; Roubaud, D.; Kristoufek, L.; Lucey, B. Bitcoin, gold, and commodities as safe havens for stocks: New insight through wavelet analysis. *Q. Rev. Econ. Financ.* **2020**, *77*, 156–164. [[CrossRef](#)]
52. Drożdż, S.; Kwapien, J.; Oświęcimka, P.; Stanisiz, T.; Wątopek, M. Complexity in economic and social systems: Cryptocurrency market at around COVID-19. *Entropy* **2020**, *22*, 1043. [[CrossRef](#)]
53. James, N. Dynamics, behaviours, and anomaly persistence in cryptocurrencies and equities surrounding COVID-19. *Physica A* **2021**, *570*, 125831. [[CrossRef](#)]
54. James, N.; Menzies, M.; Chan, J. Changes to the extreme and erratic behaviour of cryptocurrencies during COVID-19. *Physica A* **2021**, *565*, 125581. [[CrossRef](#)]
55. Wątopek, M.; Kwapien, J.; Drożdż, S. Cryptocurrencies are becoming part of the world global financial market. *Entropy* **2023**, *25*, 377. [[CrossRef](#)]
56. Binance. Available online: <https://www.binance.com/> (accessed on 1 January 2023).
57. Marketshare. Available online: <https://www.coindesk.com/markets/2023/01/04/binance-led-market-share-in-2022-despite-overall-decline-in-cex-volumes/> (accessed on 1 April 2023).
58. Tether. Available online: <https://tether.to/> (accessed on 1 January 2023).
59. Farmer, J.D.; Gillemot, L.; Lillo, F.; Mike, S.; Sen, A. What really causes large price changes? *Quant. Financ.* **2004**, *4*, 383–397. [[CrossRef](#)]
60. Drożdż, S.; Forczek, M.; Kwapien, J.; Oświęcimka, P.; Rak, R. Stock market return distributions: From past to present. *Physica A* **2007**, *383*, 59–64. [[CrossRef](#)]
61. Plerou, V.; Gopikrishnan, P.; Rosenow, B.; Nunes Amaral, L.A.; Stanley, H.E. Universal and nonuniversal properties of cross-correlations in financial time series. *Phys. Rev. Lett.* **1999**, *83*, 1471–1474. [[CrossRef](#)]
62. Drożdż, S.; Kwapien, J.; Gümmer, F.; Ruf, F.; Speth, J. Are the contemporary financial fluctuations sooner converging to normal? *Acta Phys. Pol. B* **2002**, *34*, 4293–4306.
63. Nani, A. The doge worth 88 billion dollars: A case study of Dogecoin. *Convergence* **2022**, *28*, 1719–1736. [[CrossRef](#)]
64. Shahzad, S.J.H.; Anas, M.; Bouri, E. Price explosiveness in cryptocurrencies and Elon Musk’s tweets. *Financ. Res. Lett.* **2022**, *47*, 102695. [[CrossRef](#)]
65. Dufour, A.; Engle, R.F. Time and the price impact of a trade. *J. Financ.* **2000**, *45*, 2467–2498. [[CrossRef](#)]
66. Weber, P.; Rosenow, B. Order book approach to price impact. *Quant. Financ.* **2005**, *5*, 357–364. [[CrossRef](#)]
67. Wilinski, M.; Cui, W.; Brabazon, A. An analysis of price impact functions of individual trades on the London Stock Exchange. *Quant. Financ.* **2014**, *15*, 1727–1735. [[CrossRef](#)]
68. Cont, R.; Kukanov, A.; Stoikov, S. The price impact of order book events. *J. Financ. Econom.* **2014**, *12*, 47–88. [[CrossRef](#)]
69. Kwapien, J.; Oświęcimka, P.; Drożdż, S. Detrended fluctuation analysis made flexible to detect range of cross-correlated fluctuations. *Phys. Rev. E* **2015**, *92*, 052815. [[CrossRef](#)] [[PubMed](#)]
70. Oświęcimka, P.; Drożdż, S.; Forczek, M.; Jadach, S.; Kwapien, J. Detrended cross-correlation analysis consistently extended to multifractality. *Phys. Rev. E* **2014**, *89*, 023305. [[CrossRef](#)] [[PubMed](#)]
71. Epps, T.W. Comovements in stock prices in the very short run. *J. Am. Stat. Assoc.* **1979**, *74*, 291–298.
72. Kwapien, J.; Drożdż, S.; Speth, J. Time scales involved in emergent market coherence. *Physica A* **2004**, *337*, 231–242. [[CrossRef](#)]
73. Toth, B.; Kertesz, J. The Epps effect revisited. *Quant. Financ.* **2009**, *9*, 793–802. [[CrossRef](#)]
74. Chen, J.; Lin, D.; Wu, J. Do cryptocurrency exchanges fake trading volumes? An empirical analysis of wash trading based on data mining. *Physica A* **2022**, *586*, 126405. [[CrossRef](#)]
75. Rak, R.; Drożdż, S.; Kwapien, J. Nonextensive statistical features of the Polish stock market fluctuations. *Physica A* **2007**, *374*, 315–324. [[CrossRef](#)]
76. Drożdż, S.; Kwapien, J.; Oświęcimka, P.; Rak, R. Quantitative features of multifractal subtleties in time series. *EPL* **2009**, *88*, 60003. [[CrossRef](#)]

77. Kantelhardt, J.W.; Zschiegner, S.A.; Koscielny-Bunde, E.; Havlin, S.; Bunde, A.; Stanley, H.E. Multifractal detrended fluctuation analysis of nonstationary time series. *Physica A* **2002**, *316*, 87–114. [[CrossRef](#)]
78. Zhou, W.X. Finite-size effect and the components of multifractality in financial volatility. *Chaos, Solitons Fractals* **2012**, *45*, 147–155. [[CrossRef](#)]
79. Klamut, J.; Kutner, R.; Gubiec, T.; Struzik, Z.R. Multibranch multifractality and the phase transitions in time series of mean interevent times. *Phys. Rev. E* **2020**, *101*, 063303. [[CrossRef](#)] [[PubMed](#)]
80. Garcin, M. Fractal analysis of the multifractality of foreign exchange rates. *Math. Methods Econ. Financ.* **2020**, *13–14*, 49–73.
81. Kwapień, J.; Blasiak, P.; Drożdż, S.; Oświęcimka, P. Genuine multifractality in time series is due to temporal correlations. *Phys. Rev. E* **2023**, *107*, 034139. [[CrossRef](#)] [[PubMed](#)]
82. Oświęcimka, P.; Kwapień, J.; Drożdż, S.; Górski, A.; Rak, R. Multifractal Model of Asset Returns versus real stock market dynamics. *Acta Phys. Pol. B* **2006**, *37*, 3083–3096.
83. Oh, G.; Eom, C.; Havlin, S.; Jung, W.S.; Wang, F.; Stanley, H.E.; Kim, S. A multifractal analysis of Asian foreign exchange markets. *Eur. Phys. J. B* **2012**, *85*, 1–6. [[CrossRef](#)]
84. Wątopek, M.; Drożdż, S.; Oświęcimka, P.; Stanuszek, M. Multifractal cross-correlations between the world oil and other financial markets in 2012–2017. *Energy Econ.* **2019**, *81*, 874–885. [[CrossRef](#)]
85. Jiang, Z.Q.; Xie, W.J.; Zhou, W.X.; Sornette, D. Multifractal analysis of financial markets: A review. *Rep. Prog. Phys.* **2019**, *82*, 125901. [[CrossRef](#)]
86. James, N.; Menzies, M.; Gottwald, G.A. On financial market correlation structures and diversification benefits across and within equity sectors. *Physica A* **2022**, *604*, 127682. [[CrossRef](#)]
87. Kwapień, J.; Drożdż, S. Physical approach to complex systems. *Phys. Rep.* **2012**, *515*, 115–226. [[CrossRef](#)]
88. James, N. Evolutionary correlation, regime switching, spectral dynamics and optimal trading strategies for cryptocurrencies and equities. *Phys. D* **2022**, *434*, 133262. [[CrossRef](#)]
89. Prim, R.C. Shortest connection networks and some generalizations. *Bell Syst. Tech. J.* **1957**, *36*, 1389–1401. [[CrossRef](#)]
90. Kwapień, J.; Oświęcimka, P.; Forczek, M.; Drożdż, S. Minimum spanning tree filtering of correlations for varying time scales and size of fluctuations. *Phys. Rev. E* **2017**, *95*, 052313. [[CrossRef](#)] [[PubMed](#)]
91. Chaudhari, H.; Crane, M. Cross-correlation dynamics and community structures of cryptocurrencies. *J. Comput. Sci.* **2020**, *44*, 101130. [[CrossRef](#)]
92. James, N.; Menzies, M. Collective dynamics, diversification and optimal portfolio construction for cryptocurrencies. *arXiv Prepr.* **2023**, arXiv:2304.08902.
93. Urquhart, A.; Zhang, H. Is Bitcoin a hedge or safe haven for currencies? An intraday analysis. *Int. Rev. Financ. Anal.* **2019**, *63*, 49–57. [[CrossRef](#)]
94. Manavi, S.A.; Jafari, G.; Rouhani, S.; Ausloos, M. Demythifying the belief in cryptocurrencies decentralized aspects. A study of cryptocurrencies time cross-correlations with common currencies, commodities and financial indices. *Physica A* **2020**, *556*, 124759. [[CrossRef](#)]
95. Kristoufek, L. Grandpa, Grandpa, Tell Me the One About Bitcoin Being a Safe Haven: New Evidence From the COVID-19 Pandemic. *Front. Phys.* **2020**, *8*, 296. [[CrossRef](#)]
96. Yarovaya, L.; Matkovskyy, R.; Jalan, A. The COVID-19 black swan crisis: Reaction and recovery of various financial markets. *Res. Int. Bus. Financ.* **2022**, *59*, 101521. [[CrossRef](#)]
97. Wang, P.; Liu, X.; Wu, S. Dynamic linkage between Bitcoin and traditional financial assets: A comparative analysis of different time frequencies. *Entropy* **2022**, *24*, 1565. [[CrossRef](#)]
98. Zitis, P.I.; Kakinaka, S.; Umeno, K.; Haniyas, M.P.; Stavrinides, S.G.; Potirakis, S.M. Investigating dynamical complexity and fractal characteristics of Bitcoin/US Dollar and Euro/US Dollar exchange rates around the COVID-19 outbreak. *Entropy* **2023**, *25*, 214. [[CrossRef](#)]
99. Dukascopy. Available online: <https://www.dukascopy.com/swiss/pl/cfd/range-of-markets/> (accessed on 1 January 2023).

Disclaimer/Publisher’s Note: The statements, opinions and data contained in all publications are solely those of the individual author(s) and contributor(s) and not of MDPI and/or the editor(s). MDPI and/or the editor(s) disclaim responsibility for any injury to people or property resulting from any ideas, methods, instructions or products referred to in the content.